Geochemistry Geophysics Geosystems G3
AN ELECTRONIC JOURNAL OF THE EARTH SCIENCES
Published by AGU and the Geochemical Society

Article
Volume 7, Number 12
5 December 2006
Q12P19, doi:10.1029/2006GC001291
ISSN: 1525-2027

Microstructural and geochemical perspectives on planktic foraminiferal preservation: "Glassy" versus "Frosty"

Philip F. Sexton and Paul A. Wilson
National Oceanography Centre, Southampton, School of Ocean and Earth Science, European Way, Southampton SO14 3ZH, U. K. (p.sexton@noc.soton.ac.uk)

Paul N. Pearson
School of Earth, Ocean and Planetary Sciences, Cardiff University, Main Building, Park Place, Cardiff CF10 3YE, U. K.

[1] In recent years it has become apparent that the "cool tropic paradox" of Paleogene and Cretaceous "greenhouse" climates arises because of the diagenetic alteration of tropical planktic foraminiferal calcite near the seafloor, yielding artificially high $\delta^{18}O$ values. Because the Mg/Ca compositions of foraminiferal and inorganic calcite are thought to be quite different, Mg/Ca measurements should be a sensitive way of monitoring diagenetic alteration. Here we examine the extent of diagenetic alteration of Eocene planktic foraminiferal calcite using scanning electron microscope imaging of foraminiferal test microstructures and geochemical ($\delta^{18}O$ and Mg/Ca) analyses. We compare microstructural and geochemical characteristics between given species exhibiting two contrasting states of preservation: those that appear "frosty" under reflected light and those that appear "glassy." Microstructural evidence reveals extensive diagenetic alteration of frosty foraminiferal tests at the micron scale, while $\delta^{18}O$ analyses document consistently higher $\delta^{18}O$ (and therefore lower paleotemperatures) in this material. Yet we find that $\delta^{18}O$ offsets between species in these frosty foraminiferal assemblages appear to be generally preserved, suggesting that frosty foraminifera remain valuable for generating relatively short (approximately $\leq$1 Myr) paleoceanographic time series that do not demand absolute estimates of paleotemperature. We also find that the observed increase in Mg/Ca for planktic foraminifera exhibiting diagenetic alteration (compared to glassy taphonomies) is far smaller than would be expected from the addition of inorganic calcite based on laboratory-derived Mg^{2+} partition coefficients. Our findings imply that a much lower Mg^{2+} partition coefficient controls inorganic calcite formation in deep sea sedimentary sections, in accordance with the findings of Baker et al. (1982).

Components: 12,424 words, 12 figures, 2 tables.

Keywords: planktic foraminifera; preservation; diagenesis; Eocene; stable isotopes; Mg/Ca.

Index Terms: 0419 Biogeosciences: Biomineralization; 1065 Geochemistry: Major and trace element geochemistry; 1041 Geochemistry: Stable isotope geochemistry (0454, 4870).

Received 1 March 2006; **Revised** 31 May 2006; **Accepted** 8 September 2006; **Published** 5 December 2006.

Sexton, P. F., P. A. Wilson, and P. N. Pearson (2006), Microstructural and geochemical perspectives on planktic foraminiferal preservation: "Glassy" versus "Frosty," *Geochem. Geophys. Geosyst.*, *7*, Q12P19, doi:10.1029/2006GC001291.

Theme: Development of the Foraminiferal Mg/Ca Proxy for Paleoceanography
Guest Editor: Pamela Martin

1. Introduction

1.1. "Cool Tropic Paradox"

[2] Tectonically formulated models of the geochemical carbon cycle [*Berner et al.*, 1983; *Berner*, 1994; *Tajika*, 1998; *Berner and Kothavala*, 2001; *Wallmann*, 2001] and numerical modeling experiments using General Circulation Models (GCMs) [*Sloan and Barron*, 1992; *Barron et al.*, 1993; *Sloan and Rea*, 1996; *Poulsen et al.*, 1999; *Bice and Norris*, 2002; *Shellito et al.*, 2003] have long attributed Eocene and mid-Cretaceous climatic warmth to the presence of high partial pressures of radiatively important greenhouse gases, in particular CO_2. The concept of Eocene and mid-Cretaceous atmospheres with higher-than-modern concentrations of CO_2 ($\sim$2 to 6 times the pre-industrial level) has received recent support from new indirect proxy methods for estimating atmospheric CO_2 concentrations [*Ekart et al.*, 1999; *Pearson and Palmer*, 2000; *Pagani et al.*, 2005; *Haworth et al.*, 2005]. GCMs predict that "greenhouse" intervals of elevated atmospheric carbon dioxide should be characterized by increased surface temperatures across all latitudes [*Bush and Philander*, 1997; *Huber and Sloan*, 2000, 2001; *Poulsen et al.*, 2001]. However, while reconstructions of Eocene and Cretaceous sea surface temperatures (SSTs) using $\delta^{18}O$ in planktic foraminiferal calcite have typically indicated high latitude temperatures that are substantially warmer (by 15 to 18°C) than modern [*Stott et al.*, 1990; *Barrera and Huber*, 1991; *Zachos et al.*, 1994; *Huber et al.*, 1995], tropical and subtropical reconstructions have traditionally yielded SSTs that are conspicuously cooler (by 2 to 15°C) than those of the modern low latitudes [*Douglas and Savin*, 1973, 1975; *Savin*, 1977; *Shackleton and Boersma*, 1981; *Boersma et al.*, 1987; *Horrell*, 1990; *Crowley*, 1991; *Barrera*, 1994; *Zachos et al.*, 1994; *Bralower et al.*, 1995; *Price et al.*, 1998; *Wade and Kroon*, 2002]. This apparent contradiction between GCM predictions and foraminiferal $\delta^{18}O$-derived paleotemperatures was pointed out over 20 years ago [*Manabe and Bryan*, 1985] and has since become known as the "cool tropic paradox" [*D'Hondt and Arthur*, 1996].

[3] Various explanations have been proposed to account for the cool tropic paradox (reviewed by *Crowley and Zachos* [2000]), and these have now centered on possible deficiencies in tropical planktic foraminiferal $\delta^{18}O$ data. In particular, the role of diagenetic alteration in driving foraminiferal $\delta^{18}O$ toward higher values, and therefore artificially cool $\delta^{18}O$-derived paleotemperatures, has received renewed interest in recent years [e.g., *Schrag et al.*, 1995; *Wilson and Opdyke*, 1996; *Norris and Wilson*, 1998; *Wilson and Norris*, 2001; *Pearson et al.*, 2001; *Norris et al.*, 2002; *Wilson et al.*, 2002]. Diagenetic alteration has been shown to occur predominantly at an early stage during shallow burial and, as a result of the paleoceanographic strategy of drilling unusually shallowly buried sections, with minimal influence of pore fluid chemistry [*Rudnicki et al.*, 2001]. With the advent of Mg/Ca as an independent proxy for paleotemperature, it is now possible to tackle the cool tropic paradox from a new perspective. Additionally, recent discoveries of exceptionally well preserved fossil foraminiferal calcite, combined with arrays of "typical" fossil foraminiferal assemblages from several decades of deep ocean drilling, offer an opportunity to examine the microstructural and geochemical nature of diagenetic alteration in foraminiferal calcite.

1.2. Mg/Ca in Foraminiferal Calcite

[4] As an independent paleotemperature proxy, Mg/Ca in planktic foraminiferal calcite might seem an obvious tool with which to attempt to tackle the cool tropic paradox. Indeed, reconstruction of Eocene tropical SSTs using planktic foraminiferal Mg/Ca has recently been attempted [*Tripati et al.*, 2003; *Zachos et al.*, 2003]. However, as for $\delta^{18}O$, interpretation of Mg/Ca-derived paleotemperatures is also complicated by post-depositional diagenesis. Mg/Ca in core top planktic foraminifera has been shown to be lowered through preferential removal of Mg^{2+} during early stage dissolution [*Brown and Elderfield*, 1996; *Lea et al.*, 2000; *Rosenthal et al.*, 2000; *Dekens et al.*, 2002]. However, it is the addition of secondary inorganic calcite to the foraminiferal test that has the greatest potential to change primary foraminiferal Mg/Ca values. This is because partition coefficients for

Mg^{2+} between seawater and calcite (D_{Mg}) calculated from laboratory experiments [*Winland*, 1969; *Katz*, 1973; *Mucci and Morse*, 1983; *Mucci*, 1987; *Oomori et al.*, 1987], predict that inorganic diagenetic calcite contains much more Mg^{2+} than primary biogenic foraminiferal calcite (over an order of magnitude more Mg^{2+} in inorganic calcite). The end-member Mg/Ca compositions of foraminiferal and inorganic calcite should therefore be quite different. D_{Mg} is represented by

$$D_{Mg} = (Mg/Ca)_s/(Mg/Ca)_{fl}, \quad (1)$$

where "$(Mg/Ca)_{fl}$" and "$(Mg/Ca)_s$" are the respective Mg/Ca compositions of the fluid from which the calcite precipitates and the solid calcite itself. The potential sensitivity of foraminiferal Mg/Ca to the addition of inorganic calcite presents both a hazard (to the generation of reliable down core records) and an opportunity (in theory Mg/Ca measurements should be a sensitive way to assess the addition of diagenetic calcite).

1.3. Approach

[5] Here we adopt a dual approach to assess the extent of diagenetic alteration of fossil planktic foraminiferal tests. We use Scanning Electron Microscope (SEM) imaging to examine the microstructural details of planktic foraminifera and $\delta^{18}O$ and Mg/Ca analyses to elucidate the effects of the observed diagenetic alteration on geochemical proxies for paleotemperature. We present multispecies data for eight samples from Eocene drill sites with tropical and subtropical locations hosting foraminifera with two distinctly different taphonomies: "glassy" and "frosty" (see section 2). One method for developing a more quantitative estimate of the extent of diagenetic alteration is to compare the geochemical compositions of secondary inorganic calcite and primary biogenic calcite. With information on the overall geochemical composition of the diagenetically altered whole foraminiferal test, the relative contributions of both of these two calcite sources can then be estimated by mixing ratios. There is great potential for application of ion probe or laser ablation mass spectrometric techniques to derive the end-member composition of secondary inorganic calcite [e.g., *Allison and Austin*, 2003; *Eggins et al.*, 2003; *Hathorne et al.*, 2003; *Reichart et al.*, 2003], but these methods are relatively new, and with respect to measurement of $\delta^{18}O$ in calcite, are imprecise. Here we take a different approach by using down core pore fluid [Mg^{2+}] and [Ca^{2+}] data at ODP Site 1052 to estimate the Mg/Ca composition of inorganic calcite, contemporaneous with in situ diagenetically altered middle Eocene planktic foraminifera.

2. Diagenesis of Foraminiferal Calcite: Terminology

[6] A distinction must be made between different styles of diagenetic alteration. We advocate the use of more specific terminology to describe the various distinct styles of diagenetic alteration, such as that introduced by *Folk* [1965]. The term "neomorphism" describes the process of replacement of a particular mineral (e.g., biogenic calcite) by the same mineral but with different crystal form (e.g., inorganic calcite). The term "recrystallization" was first used in relation to carbonates to describe this process [*Sorby*, 1879]. However, here we choose to use the term "neomorphism" for clarity because "recrystallization" is often used loosely in the micropaleontological and paleoceanographic literature to describe all forms of diagenetic alteration of biogenic calcite. A second conspicuous diagenetic process in carbonates is the addition of new inorganic calcite, which can be defined by the term "cementation." Growth of inorganic calcite crystals during cementation can occur across a spectrum of crystal sizes, from micron-scale rhombs of inorganic calcite, or "overgrowths," to much larger-scale "infilling" of foraminiferal chambers.

[7] Living non-encrusting planktic foraminifera are translucent ("glassy"), whereas fossil planktic foraminifera typically have a "frosty" appearance. It has been suggested that the absence of a glassy appearance in fossil foraminiferal tests is likely a consequence of diagenetic alteration at the micron-scale [*Pearson et al.*, 2001]. The nature of this alteration becomes abundantly clear in detailed SEM images (Figure 1; see "enhanced" high-resolution figure in the HTML version). These images show extensive micron-scale cemented overgrowths covering the test. Additionally, diagenetic alteration of foraminiferal tests may involve neomorphism of primary biogenic calcite. The presence of overgrowths and/or neomorphic calcite are impossible to see directly under the binocular microscope. Foraminifera altered in this manner commonly retain microstructural features such as wall pores and surface ornamentation, and this fact has led many workers to assume that frosty material such as that shown in Figure 1 is "well preserved." However, evidence has been mounting that casts doubt on this assertion. Specifically, the

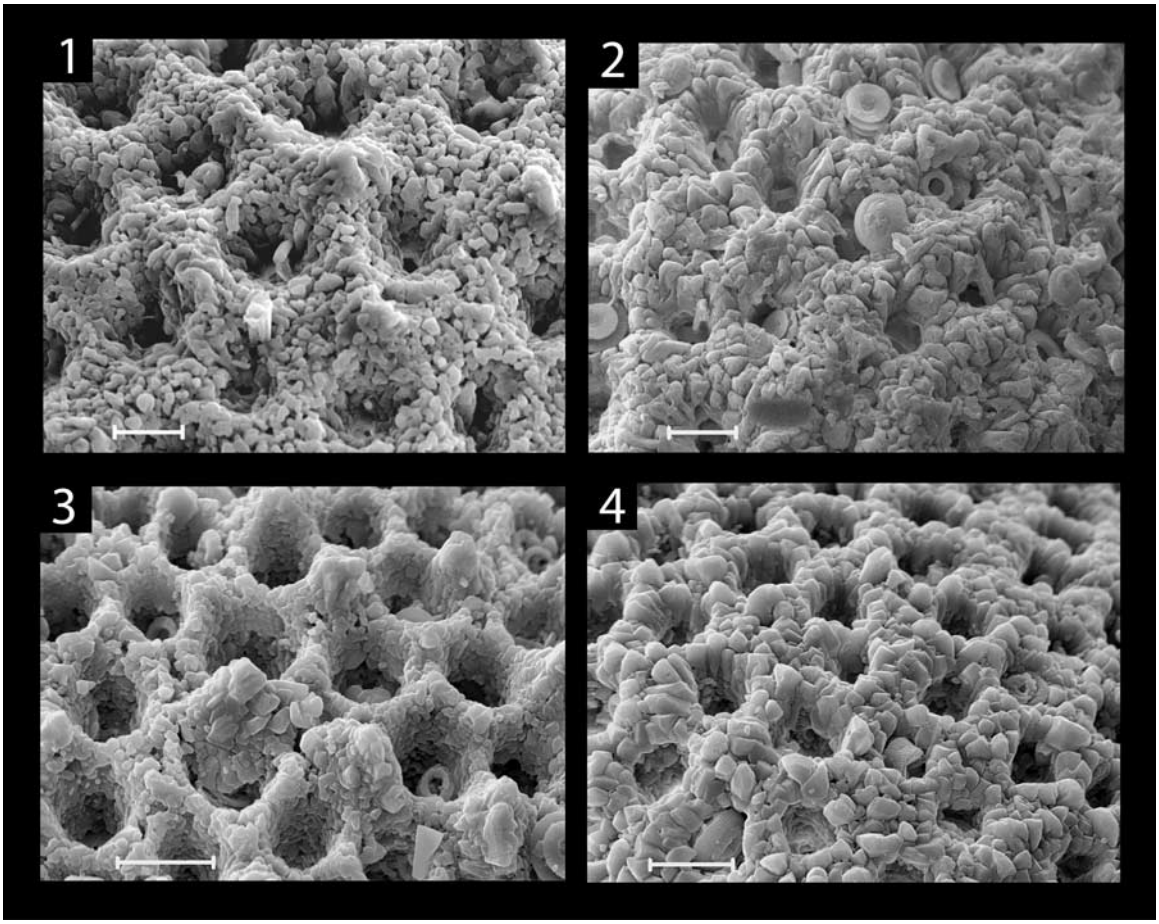

Figure 1. Detailed images of the wall textures of "frosty" middle Eocene planktic foraminifera from "typical pelagic" ODP drill sites. "Frosty" denotes their appearance when viewed using a binocular microscope and contrasts with exceptionally well preserved foraminifera that appear "glassy." Images of these frosty foraminifera reveal an abundance of micron-scale cemented overgrowths covering the tests. These micron-scale overgrowths are impossible to see directly under the binocular microscope. Images 1 and 2 are from ODP Site 1052; images 3 and 4 are from ODP Site 865. All specimens are from biozone E13 (~39 Ma). Samples studied are as follows: 1, 1052B 10H-2, 133–136 cm; 2, ODP 1052B, 11H-4, 3–6 cm; 3 and 4, ODP 865, 4H-4, 110–112 cm. Image 1 is also reproduced as Figure 2g of *Pearson et al.* [2001]. All scale bars are 10 μm. Also available online as an "enhanced" high-resolution figure in the HTML version.

translucent, "glassy" appearance (similar to modern living foraminifera) of Cretaceous and Eocene planktic foraminifera recovered from hemipelagic clay-rich sediments [*Norris and Wilson*, 1998; *Wilson and Norris*, 2001; *Pearson et al.*, 2001; *Norris et al.*, 2002; *Wilson et al.*, 2002] supports the view that much of the frosty material is, in fact, significantly altered. The terms "glassy" and "frosty" imply two end-member taphonomies, but in reality there is probably a continuum of intermediate states of preservation in between. Additionally, foraminiferal calcite that we describe here as "frosty" has undergone relatively modest diagenetic alteration while material that has progressed further through the alteration process could be described as "chalky."

[8] The exceptional preservation of foraminiferal tests from "hemipelagic" clay-rich settings (hereafter synonymous with "glassy" taphonomy) has been attributed to the impermeable nature of the clay-rich sediments preventing interaction of the foraminiferal calcite with surrounding pore waters [*Norris and Wilson*, 1998; *Wilson and Norris*, 2001; *Pearson et al.*, 2001; *Wilson et al.*, 2002]. In contrast, the more permeable sediments of "typical pelagic" open ocean settings (hereafter synonymous with "frosty" taphonomy) apparently lead to poorer preservation because of greater chemical interaction between foraminiferal calcite and pore waters. Despite the well-preserved nature of foraminiferal calcite from hemipelagic settings, these locations are, by their nature, toward the

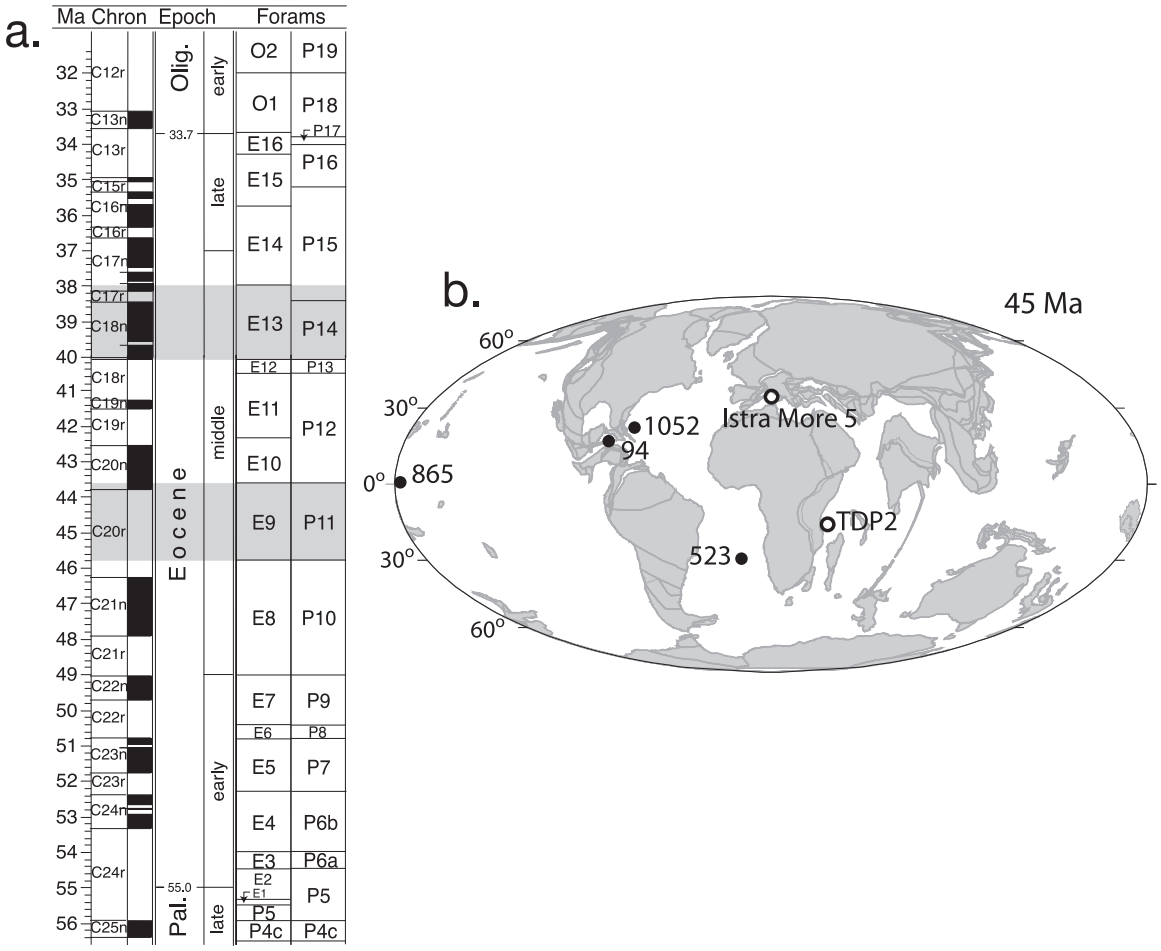

Figure 2. (a) Magnetobiostratigraphic timescale for the Eocene Epoch (numerical timescale of *Berggren et al.* [1995]). New biozonation scheme using "E" zones is from *Berggren and Pearson* [2005], while that using "P" zones is from *Berggren et al.* [1995]. Gray shading shows the stratigraphic positions of the two middle Eocene time slices studied (planktic foraminiferal biozones E9 and E13). (b) Paleogeographic reconstruction for the early middle Eocene (~45 Ma) showing the location of drill sites discussed in this article. Paleogeographic map from the Ocean Drilling Stratigraphic Network (ODSN) Plate Tectonic Reconstruction Service (http://www.odsn.de/odsn/services/paleomap/paleomap.html). Open circles denote sites with hemipelagic clay-rich lithologies; solid dots denote sites with "typical pelagic" carbonate-rich lithologies.

peripheries of ocean basins. The diversity of objectives that fuel paleoceanography dictate that the majority of ocean drilling has, and will probably continue to be, conducted in typical pelagic open ocean settings where carbonate-bearing clay-rich sediments are extremely rare. Hence it is important to understand the nature and magnitude of geochemical alteration in frosty foraminiferal calcite.

3. Site Locations and Stratigraphies

[9] Data are presented from two time slices within the middle Eocene: planktic foraminiferal biozones E9 (= P11 using "P" zonation) (~45 Ma) and E13 (= P14/lower P15 using "P" zonation) (~39 Ma) (Figure 2a), using four different samples within each biozone. We use the new Eocene planktic foraminifer zonation ("E" zones) of *Berggren and Pearson* [2005] but provide correlation to the "P" zones of *Berggren et al.* [1995] for continuity. Samples are from various Deep Sea Drilling Project (DSDP), Ocean Drilling Program (ODP) and other drill sites (Table 1 and Figure 2b). Data are presented from hemipelagic, clay-rich sites hosting extremely well preserved "glassy" planktic foraminifera and from so-called "typical pelagic," carbonate-rich depositional settings hosting planktic foraminifera with a "frosty" taphonomy.

[10] Ideally, an experiment designed to test the effect of diagenesis on geochemical signatures in

Table 1. Drill Sites Used[a]

Site	Paleodepth, mbsl	Spl Depth (in Core), mbsf	Paleolatitude	Lithology
Biozone E9 (~45 Ma)				
TDP 2	Slope/Bathyal	36	18°S	clay
DSDP 94	Bathyal	490	19°N	foram-nannofossil ooze
DSDP 523	3000	161	32°S	marly nannofossil ooze
ODP 865	1300–1500	70	4°N	foram-nannofossil ooze
Site	Paleodepth, mbsl	Spl Depth (in Core), mbsf	Paleolatitude	Lithology
Biozone E13 (~39 Ma)				
Istra More 5	Slope	1170	42°N	silty marl
ODP 865	1300–1500	28	5°N	foram-nannofossil ooze
ODP 1052F	~1000	97	22°N	siliceous nannofossil ooze
ODP 1052B	~1000	86	22°N	siliceous nannofossil ooze

[a] Abbreviations: mbsl, meters below sea level; mbsf, meters below seafloor; TDP, Tanzania Drilling Project; Spl, sample.

planktic foraminiferal calcite would utilize a single sedimentary section with high frequency, rhythmic variations in lithology that give rise to rhythmic variations in foraminiferal taphonomy. Unfortunately, a section of this type is not available. Instead, the use of multiple sites (with contrasting taphonomies) demands that a balance must be made between the desire to document variability across the spectrum of planktic foraminiferal taphonomy and the desire to restrict the sites used to as narrow a latitudinal band as possible to minimize inter-site differences in surface ocean paleotemperatures that affect primary $\delta^{18}O$ and Mg/Ca signals. Because of the relatively poor spatial density of drill sites in the Eocene, sites are chosen with paleolatitudes between ~30° north or south of the paleoequator for both time slices (with the exception of one site located at 42°N). Nevertheless, two of the four samples from late middle Eocene biozone E13 were chosen because they contained contrasting planktic foraminiferal taphonomies (as identified under reflected light) at a single site (ODP Site 1052, Hole F = taphonomically similar to other frosty material analyzed here; Site 1052, Hole B = noticeably poorer state of preservation). However, comparing their constituent foraminifera visually (in detail using SEM imaging) and geochemically ($\delta^{18}O$ and Mg/Ca) did not reveal any significant differences.

4. Methods

[11] Sediment samples (~20 cc volume) were disaggregated by soaking in deionized water for 30 min and wet-sieving through a 63 μm mesh. Foraminifera were picked from narrow ($\leq$50 μm) size fractions within the 212–400 μm size range. Scanning electron micrographs were generated using a Leo 1450VP (variable pressure) digital SEM fitted with a tungsten filament. Prior to SEM analysis, foraminiferal specimens were gold coated. Gold coating optimizes the backscattering of secondary electrons from the sample, providing better topographic imaging. Occasionally, foraminiferal specimens exhibited "charging," the generation of an excessively bright image. Interestingly, charging was more common in material with a poorer state of preservation.

[12] Stable isotope ratios were analyzed for monospecific samples using a Europa Geo 20–20 mass spectrometer equipped with a "CAPS" automatic carbonate preparation system. Between 6 and 14 specimens were analyzed from the relevant size fraction after cleaning ultrasonically in deionized water. Results are reported relative to the Vienna Peedee Belemnite standard (VPDB). Standard external analytical precision, based on replicate analysis of in-house standards calibrated to NBS-19, is better than ±0.08‰ for $\delta^{18}O$ and $\delta^{13}C$.

[13] Foraminiferal tests analyzed for trace metal contents require rigorous cleaning prior to analysis to remove contaminants. Before cleaning, picked foraminiferal tests were gently broken open between two glass plates. Foraminiferal tests were then cleaned using a protocol similar to that of *Boyle and Keigwin* [1985] but with the reductive cleaning step (designed to remove any metal oxide coatings) omitted. This latter step was omitted on the grounds that metal oxide coatings are thought not to be a major source of Mg^{2+} contaminant and the reducing reagent is corrosive to carbonate, causing partial dissolution of the sample. Samples

cleaned by protocols including the reductive step yield consistently lower Mg/Ca values (by an average 15%) than those cleaned by protocols omitting this step [*Barker et al.*, 2003]. Because the effect of partial dissolution on foraminiferal calcite is known to lower Mg/Ca ratios [*Brown and Elderfield*, 1996; *Rosenthal et al.*, 2000; *Dekens et al.*, 2002], it is therefore uncertain as to whether the lower Mg/Ca ratios in samples cleaned using the reductive step arise from removal of Mg^{2+} adhering to metal oxides or from partial dissolution of biogenic calcite. Therefore, because one key aspect of this study is to determine Mg/Ca values of foraminifera displaying different preservation states, we chose to omit this reductive step. The modified cleaning method employed here removes clays and organic matter with a final weak acid "polish" to remove any re-adsorbed contaminants. Foraminiferal samples were analyzed using a Perkin Elmer Optima 4300DV Inductively Coupled Plasma–Optical Emission Spectrometer (ICP-OES). External precisions of better than 0.21% (1σ) are obtained for Mg/Ca from dilute solutions containing between 1 and 5 ppm Ca^{2+} [e.g., *Green et al.*, 2003].

5. Middle Eocene Planktic Foraminiferal Taphonomy: Microstructure

5.1. Whole Test Taphonomy

[14] Figures 3 and 4 illustrate a selection of the planktic foraminiferal faunas from the eight samples within biozones E9 and E13. The species illustrated here do not represent all of those analyzed for their stable isotope or trace element compositions (section 6), but are simply the species common to all drill sites within each biozone. The planktic foraminifera recovered at all sites are broadly typical for contemporaneous tropical and subtropical faunas of the middle Eocene. We base our taxonomy on a new taxonomic atlas that revises the synonymy, diagnosis and description of Eocene planktic foraminifera [*Pearson et al.*, 2006]. Additionally, several previously unidentified species are found at some of the sites, in particular those from late middle Eocene biozone E13 (see *Sexton* [2005] and *Sexton et al.* [2006] for taxonomic discussions).

[15] When viewed under the light microscope, the difference in appearance between tests from hemipelagic settings and those from typical pelagic settings is particularly striking; hemipelagic foraminifera (Istra More 5 and TDP 2) have a "glassy" appearance, in contrast to typical pelagic foraminifera (the various DSDP and ODP Sites), which appear "frosty." The better preservation of the glassy planktic foraminiferal tests from the Istra More 5 and TDP 2 hemipelagic drill sites is also evident from the SEM images (Figures 3 and 4; see "enhanced" high-resolution figures in the HTML version). This disparity in preservation is illustrated by the fact that the pores of glassy individuals from the two hemipelagic sites (Figure 3, TDP 2; Figure 4, Istra More 5) are generally larger and more clearly defined compared to those of frosty individuals from the typical pelagic sites (Figure 3, DSDP 523, DSDP 94, ODP 865; Figure 4, ODP 865, ODP 1052F, ODP 1052B). Similarly, the apertures of these same glassy individuals from TDP 2 (Figure 3) and Istra More 5 (Figure 4) reveal an absence of the slight infilling of chamber interiors that frosty specimens often display.

[16] A "peeling" effect is also evident in some frosty specimens, and is most marked in species of *Turborotalia* (Figure 4, *T. pomeroli*/*T. cerroazulensis* from ODP 865, 1052F and 1052B). This peeling phenomenon (see *Hemleben and Olsson* [2006] for further discussion) is characterized by removal of the outer surface of the test, obliterating the original pore structure and exposing the earlier wall layers which have less topographic relief. Peeling is a mechanical phenomenon, possibly occurring during sample washing, but appears to be most problematic in material weakened by dissolution.

5.2. Wall Surface Textures

[17] Figures 5 and 6 (see "enhanced" high-resolution figures in the HTML version) show detailed images of the wall texture of the same foraminiferal specimens displayed in Figures 3 and 4. These wall texture images reveal a very well preserved, unaltered biogenic texture in the glassy foraminifera from hemipelagic sites TDP 2 (Figure 5) and Istra More 5 (Figure 6). In contrast, the foraminifera with a frosty appearance found in the typical pelagic DSDP and ODP drill sites possess abundant calcite overgrowths (Figure 6, figures from DSDP 523, DSDP 94, ODP 865; Figure 6, figures from ODP 865, 1052F and 1052B). These overgrowths are micron-scale rounded crystallites that frequently obscure the original surface wall texture seen in the glassy hemipelagic material. Larger ($\sim$4 to 10 μm), coarser crystallites occur on the inter-pore ridges of some frosty individuals (e.g., Figure 5, panels 3, 7, 12, 20; Figure 6, panels 7, 11, 12, 14, 18, 22, 26, 30, 32; indicated by arrows). These coarser crystallites form accentuated

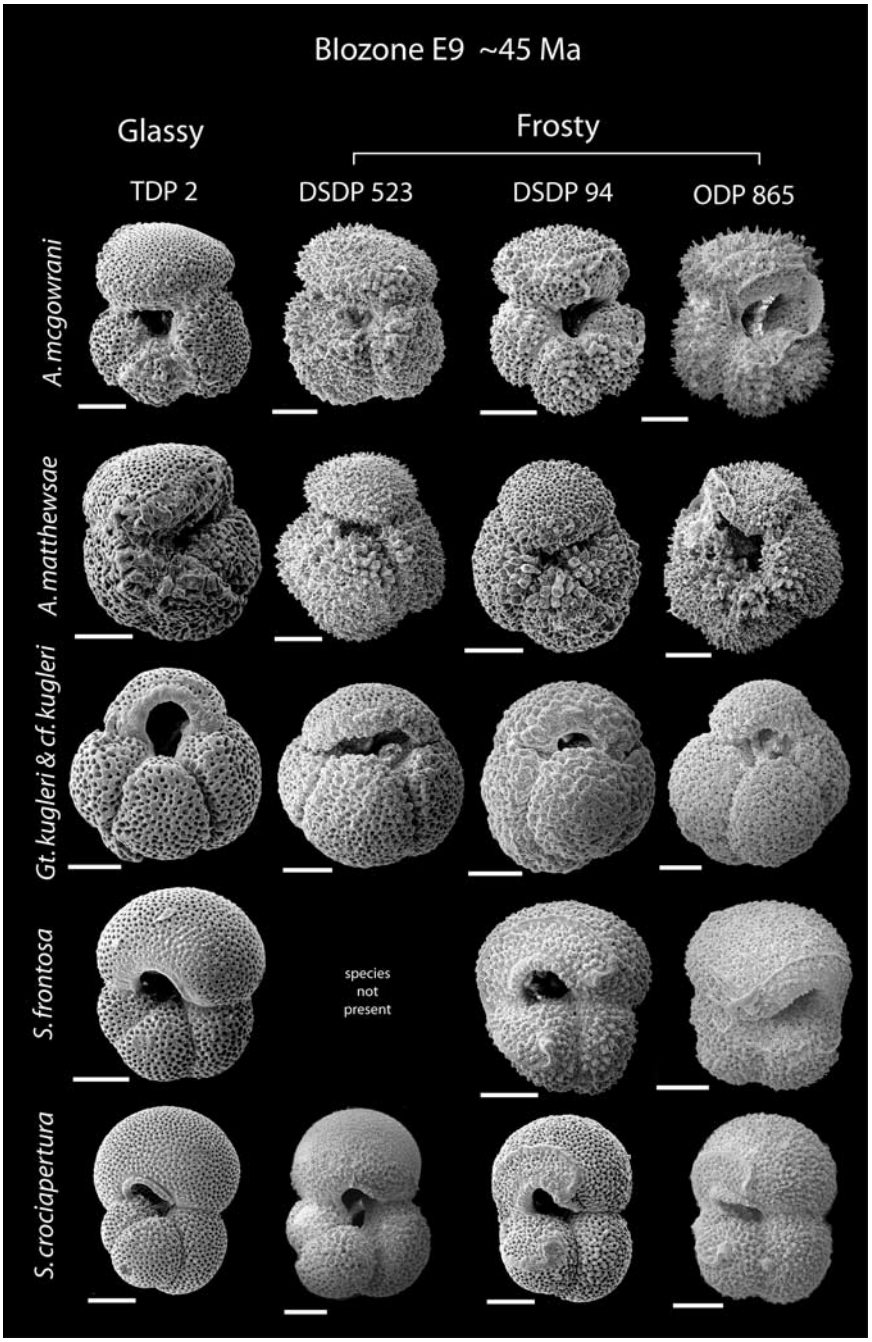

Figure 3. Planktic foraminiferal fauna from biozone E9 (~45 Ma). The five species that were present at all four sites (TDP 2, DSDP 94, DSDP 523, and ODP 865) are shown here. Samples studied are as follows: TDP 2, 15-CC; DSDP 94, 18-1, 50-52 cm; DSDP 523, 44-2, 2-4 cm; ODP 865, 8H-1, 60-62 cm. The overall better preservation of the glassy planktic foraminiferal tests from the hemipelagic TDP 2 drill site is evident from these images. All scale bars are 100 μm. *A*., *Acarinina*; *Gt*., *Globigerinatheka*; *S*., *Subbotina*. Also available online as an "enhanced" high-resolution figure in the HTML version.

blade-like "towers" on specimens of *A. mcgowrani* and *A. matthewsae* from biozone E9 (Figure 5, panels 2 and 8; indicated by arrows). These towers appear to be diagenetically altered "muricae" (delicate biogenic pustulose projections) that characterize species from the genus *Acarinina*. It is possible that the raised inter-pore ridges may serve as focal points for cementation, as may the biogenic muricae of *A. mcgowrani* and *A. matthewsae*. Support for this idea is provided by the absence of delicate biogenic muricae on glassy specimens of *A. mcgowrani* and *A. matthewsae* at the hemipelagic sites, as revealed

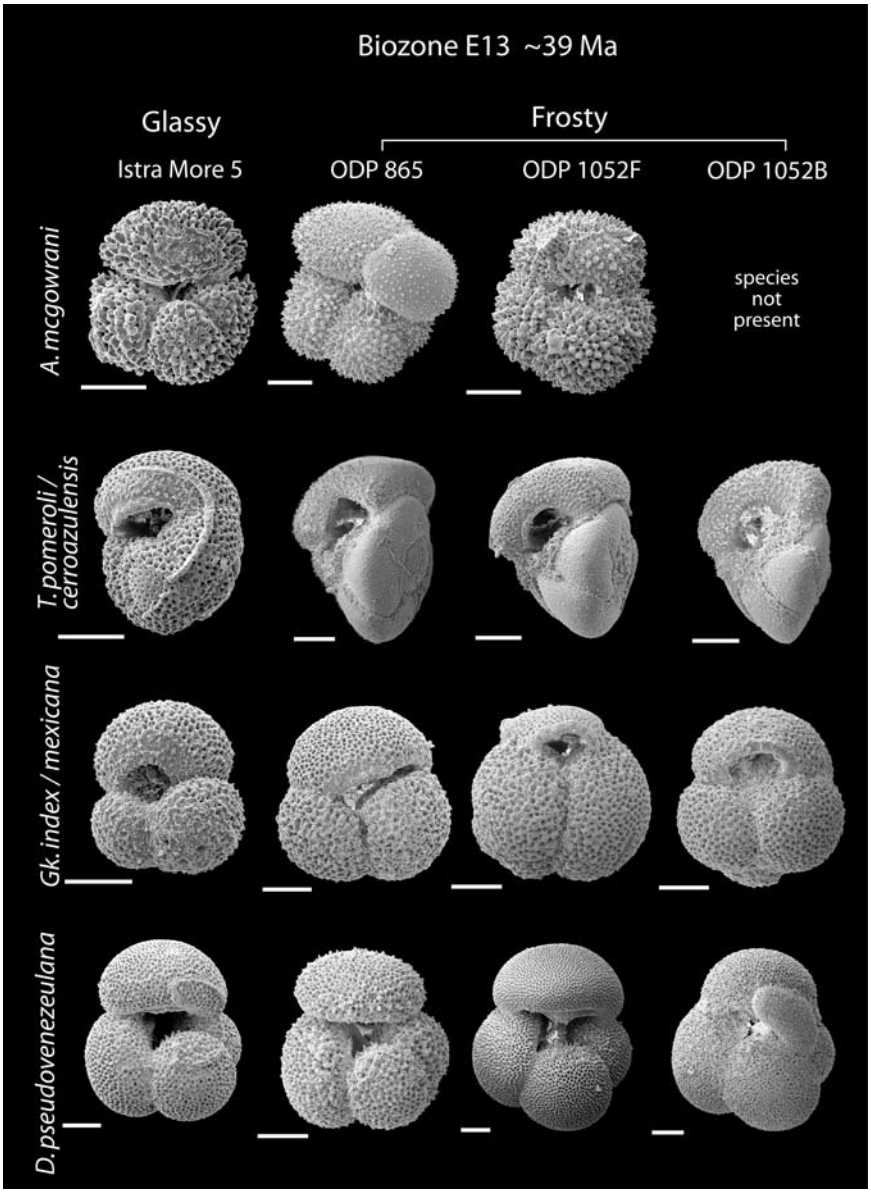

Figure 4. Planktic foraminiferal fauna from biozone E13 (~39 Ma). The eight species that were present at all four sites (Istra More 5, ODP 865, ODP 1052F and ODP 1052B) are shown here. Samples studied are as follows: Istra More 5 drill site, 1170 m; ODP 865, 4H-4, 110–112 cm; ODP 1052F, 11H-5, 83–86 cm; ODP 1052B, 11H-4, 3–6 cm. The overall better preservation of the glassy planktic foraminiferal tests from the hemipelagic Istra More 5 drill site is evident from these images. All scale bars are 100 μm. *A.*, *Acarinina*; *T.*, *Turborotalia*; *Gk.*, *Globigerinatheka*; *D.*, *Dentoglobigerina*; *S.*, *Subbotina*; *C.*, *Catapsydrax*; *P.*, *Parasubbotina*. Also available online as an "enhanced" high-resolution figure in the HTML version.

by their stubby, broken stumps (Figure 5, panels 1 and 5; Figure 6, panel 1; indicated by arrows). It is likely that the absence of these delicate projections in glassy material is caused by a mechanical process, probably sample washing.

5.3. Wall Cross Sections

[18] Planktic foraminiferal wall cross sections are examined for two species within each biozone. A mixed layer dweller and a deeper thermocline dweller are chosen to provide a contrast in depth habitats and therefore also in the environment within which the primary calcite was secreted; *A. mcgowrani* represents a mixed layer species in both biozones, while *S. crociapertura* (biozone E9) and *S. linaperta* (biozone E13) calcified in the lower thermocline [*Pearson et al.*, 1993, 2001; *Sexton et al.*, 2006]. The SEM images of test wall cross sections in glassy material from TDP 2 and

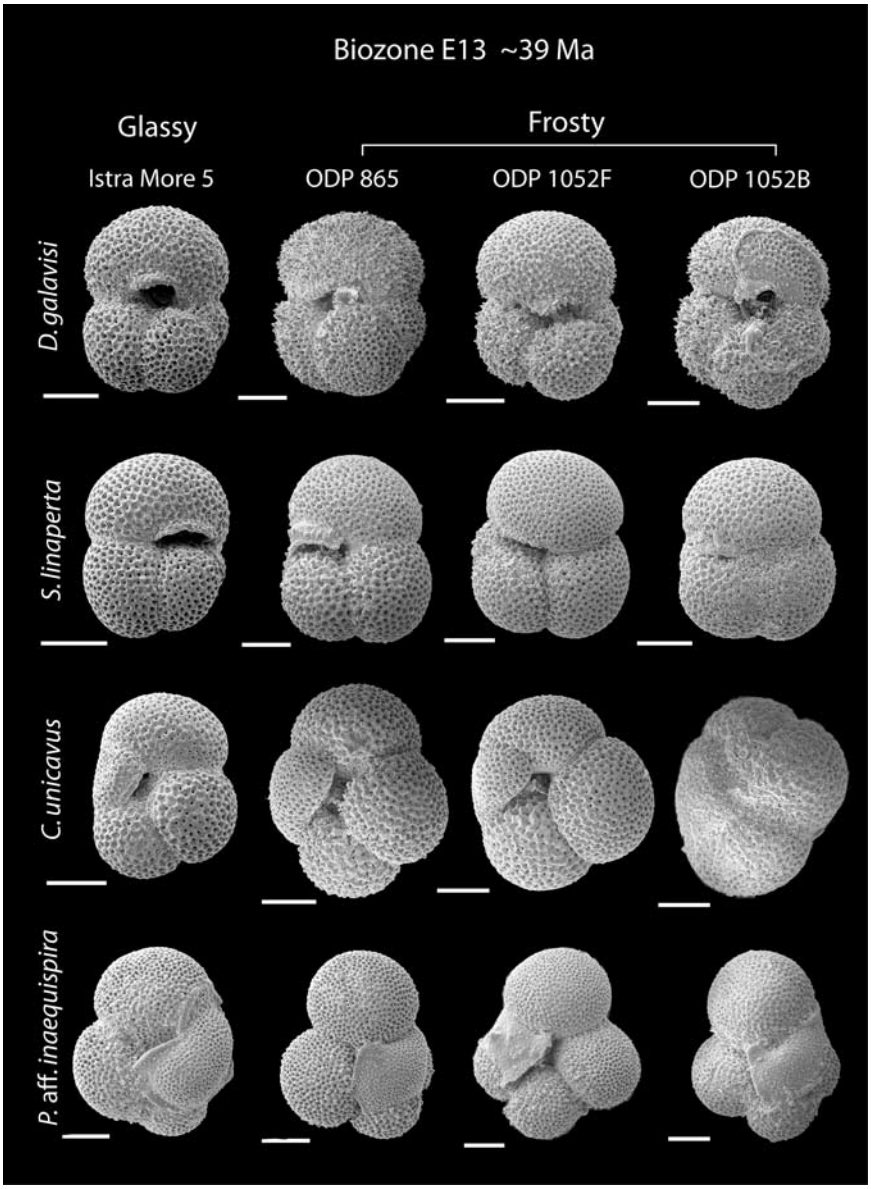

Figure 4. (continued)

Istra More 5 show planktic foraminiferal fragments that display the microgranular texture that is characteristic of biogenic calcite in Recent planktic foraminifera (Figure 7, panels 1 and 5; Figure 8, panels 1 and 5; see "enhanced" high-resolution figures in the HTML version). A cross section of one of the earlier-formed chambers of the last whorl in *A. mcgowrani* from Istra More 5 shows the vertical layering of successive chambers as new chambers are added on top of previously formed ones (Figure 8, panel 1). The site of initial calcification in planktic foraminifera, which corresponds to the original Primary Organic Membrane (POM), is commonly found two thirds of the way down from the outer test surface and is particularly clear in *S. crociapertura* from TDP 2 (Figure 7, panel 5; indicated by arrows).

[19] The presence of micron-scale overgrowths evident in the wall surface texture images of frosty foraminifera from DSDP and ODP "typical pelagic" material (Figures 5 and 6) is also clearly seen in their respective wall cross sections (Figures 7 and 8). In these wall cross sections, because some of these "overgrowths" are present on the broken surfaces of the test (instead of on the sides of the hollow pore pits), they may in fact be neomorphic in origin. Where these overgrowths/neomorphic calcite are pervasive they obscure the relief of the vertical pore pits. Despite this, the site of initial

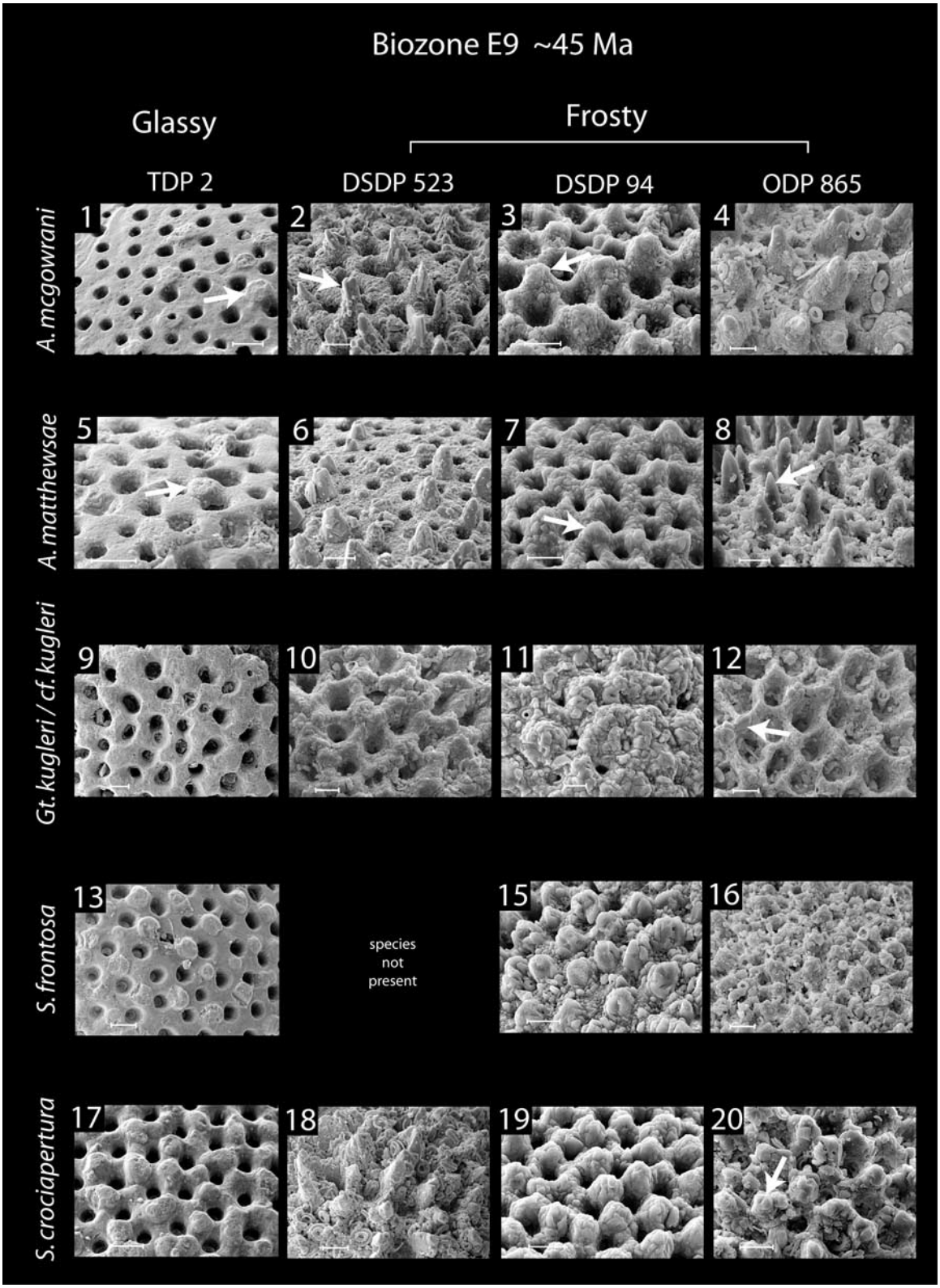

Figure 5. Detailed images of the wall textures of the same planktic foraminiferal specimens from biozone E9 as displayed in Figure 3. The very well preserved, unaltered surface texture in the glassy specimens from hemipelagic site TDP 2 is evident. By contrast, however, the same respective species found in the "typical pelagic" DSDP and ODP drill sites display varying amounts of secondary calcite covering their walls. All scale bars are 10 μm. Also available online as an "enhanced" high-resolution figure in the HTML version.

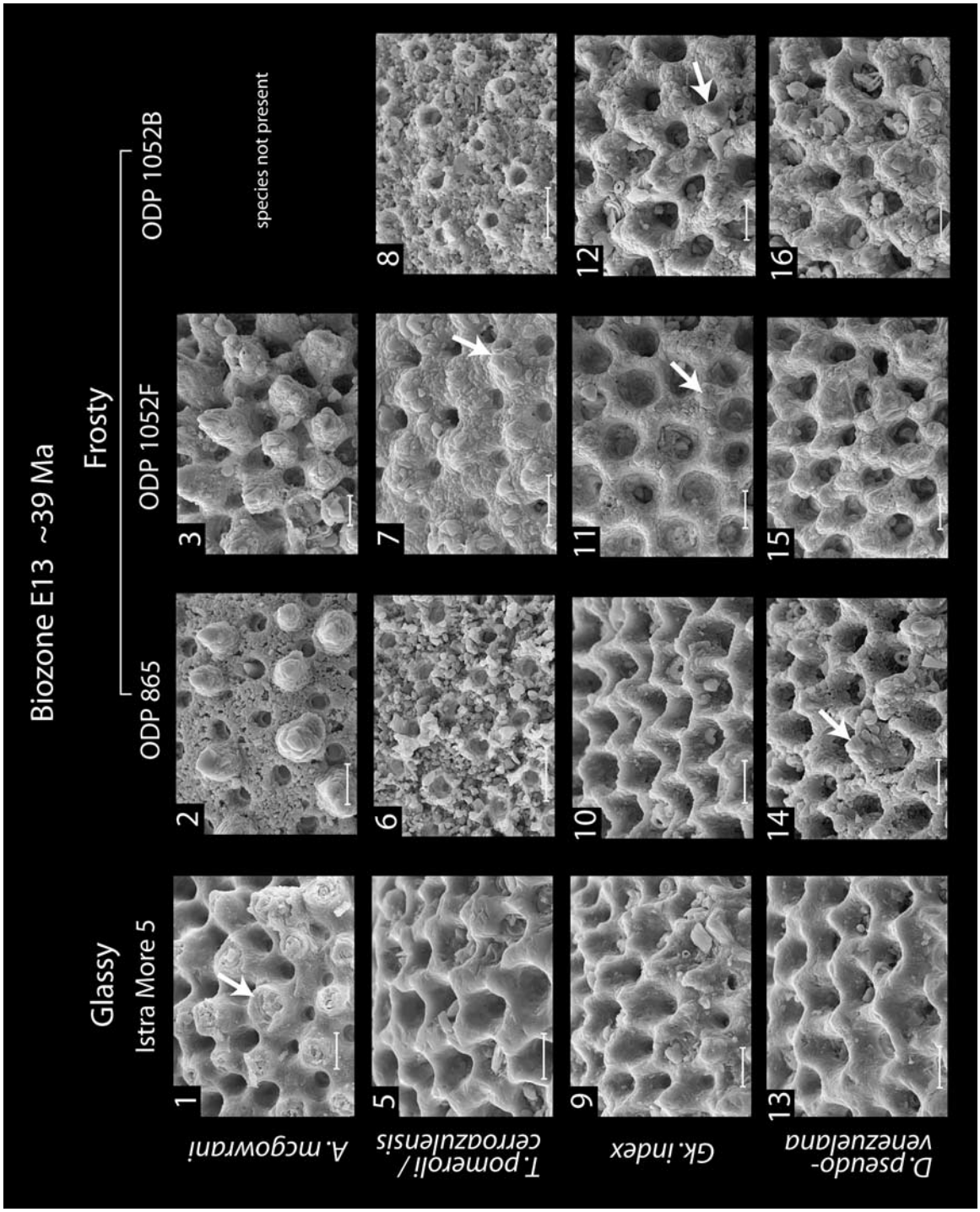

Figure 6. Detailed images of the wall textures of the same planktic foraminiferal specimens from biozone E13 as displayed in Figure 4. The very well preserved, unaltered surface texture in the glassy specimens from hemipelagic site Istra More 5 is evident. By contrast, however, the same respective species found in the "typical pelagic" ODP drill sites display varying amounts of secondary calcite covering their walls. All scale bars are 10 μm. Also available online as an "enhanced" high-resolution figure in the HTML version.

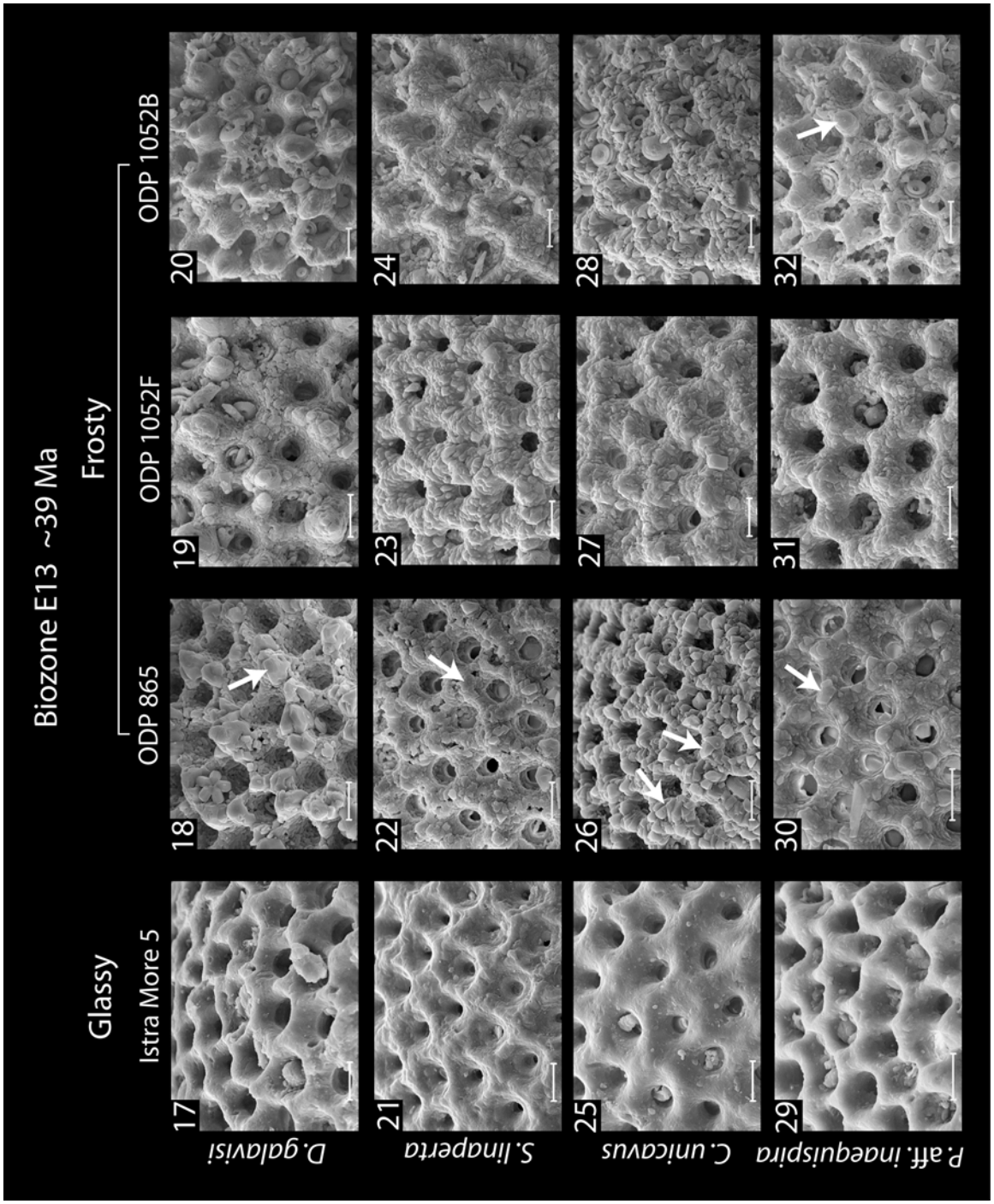

Figure 6. (contitued)

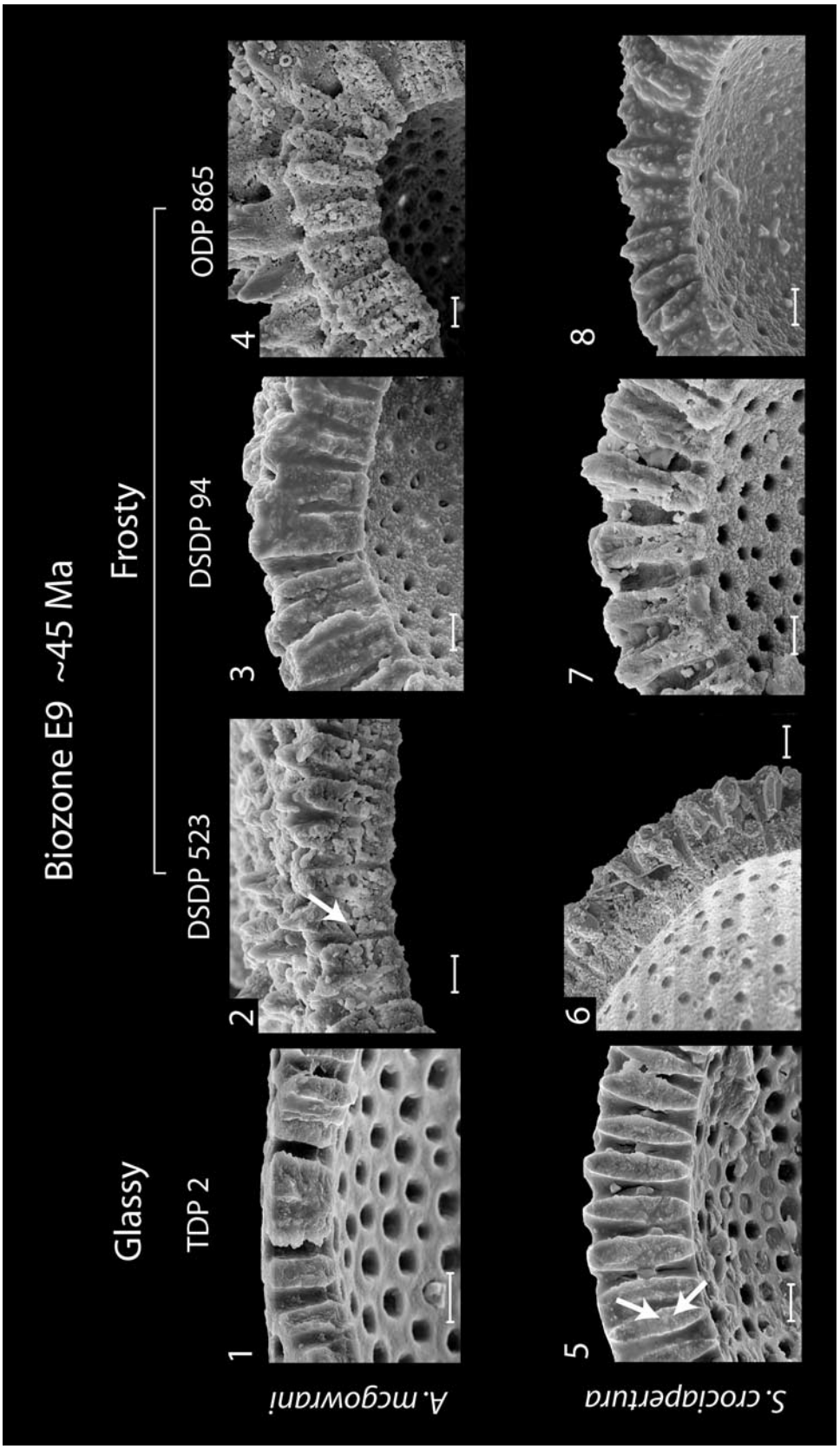
Biozone E9 ~45 Ma
Glassy
Frosty
TDP 2
DSDP 523
DSDP 94
ODP 865
A. mcgowrani
S. crociaperturа
1
2
3
4
5
6
7
8

Figure 7

calcification is often still discernible in frosty material (e.g., Figure 7, panel 2; Figure 8, panel 2; indicated by arrows). Another feature of these diagenetically altered foraminifera that suggests the presence of neomorphic calcite (and/or dissolution) is the "weathered," "melted" appearance of the pore walls in cross section (Figure 7, panels 3 and 8; Figure 8, panels 3, 6, and 7). The abundance of overgrowths across the surface of the test (Figures 5 and 6) and neomorphic calcite/overgrowths within the interior of the test (as revealed by the broken wall cross sections, Figures 7 and 8) indicate that diagenetic alteration of frosty foraminiferal calcite is not a phenomenon merely restricted to the test surface but is, in fact, pervasive throughout the test.

6. Middle Eocene Planktic Foraminiferal Taphonomy: Geochemistry

6.1. Stable Isotope Data

[20] The temperature dependence of oxygen isotope fractionation between ambient water and foraminiferal calcite during calcification means that depth-stratified foraminiferal assemblages from open ocean sites can be expected to exhibit a trend of increasing foraminiferal $\delta^{18}O$ with depth that parallels the trend of decreasing temperature [*Fairbanks et al.*, 1980, 1982]. In contrast, foraminiferal $\delta^{13}C$ decreases with depth because of the preferential uptake of $^{12}CO_2$ during photosynthesis in the surface euphotic zone and its subsequent remineralization back into the ΣCO_2 pool by respiration at depth. This basic pattern in foraminiferal $\delta^{18}O$ and $\delta^{13}C$ with water column depth facilitates the reconstruction of fossil foraminiferal depth habitats based on the relative stable isotope offsets between species in an assemblage [see *Spero*, 1998; *Pearson*, 1998; *Pearson et al.*, 2001, Figure 1]. However, $\delta^{18}O$ and $\delta^{13}C$ values can be offset from "equilibrium" with ambient seawater by the effect on isotope fractionation of environmental parameters such as $[CO_3^{2-}]$ and *p*H [*Spero et al.*, 1997; *Zeebe*, 1999] or physiological processes such as symbiont photosynthesis or foraminiferal respiration [*Spero and Williams*, 1989; *Spero et al.*, 1991; *Spero and Lea*, 1993, 1996]. Although the combined effect of physiologically driven disequilibrium $\delta^{13}C$ fractionation in planktic foraminifera probably attenuates the inferred gradient of upper water column $\delta^{13}C$ of ΣCO_2 [*Ortiz et al.*, 1996], it appears that the combined effect of these "disequilibrium" processes generally has less of an effect on foraminiferal calcite $\delta^{18}O$ and $\delta^{13}C$ than changes in upper water column temperature and $\delta^{13}C$ of ΣCO_2 [*Ortiz et al.*, 1996].

[21] For each drill site in each biozone, all planktic foraminiferal species that were sufficiently abundant were analyzed for $\delta^{18}O$ and $\delta^{13}C$. Data are shown as stable isotope crossplots for biozones E9 (Figure 9) and E13 (Figure 10). The inferred relative depth stratification of the planktic foraminifera is consistent with the conclusions drawn from a variety of other Eocene studies [*Poore and Matthews*, 1984; *Shackleton et al.*, 1985; *Boersma et al.*, 1987, *Stott et al.*, 1990; *Pearson et al.*, 1993, 2001; *Coxall et al.*, 2000; *Sexton et al.*, 2006]. Figures 9 and 10 show that within each biozone, given species of frosty planktic foraminifera from typical pelagic sites (black framed plots) display similar $\delta^{18}O$ values. However, within each biozone, the absolute $\delta^{18}O$ values of these frosty species are offset to higher values compared to those same (glassy) species from the corresponding hemipelagic sites (TDP 2 and Istra More 5; red framed plots).

[22] This intraspecies $\delta^{18}O$ offset between drill sites appears to be relatively constant; within biozone E9, $\delta^{18}O$ values for species from the three typical pelagic samples are consistently about 2.0‰ higher compared to those same species from the hemipelagic sample (TDP 2). Similarly, within biozone E13, species in the three typical pelagic samples register $\delta^{18}O$ values approximately 1.2‰ higher than those same species from the hemipelagic sample (Istra More 5). In light of the SEM evidence showing pervasive diagenetic alteration (Figures 5 to 8), the most plausible explanation for the relatively large and consistent $\delta^{18}O$

Figure 7. Detailed images of the wall cross sections of two planktic foraminiferal species (*A. mcgowrani*, a mixed layer dweller, and *S. crociapertura*, a deeper thermocline dweller) from biozone E9. Foraminifera were taken from the same samples as those used for Figures 3 and 5. The broken glassy tests from TDP 2 display the microgranular texture that is characteristic of biogenic calcite in Recent planktic foraminifera. Micron-scale diagenetic alteration in the broken frosty tests from "typical pelagic" DSDP and ODP drill sites is evident, even obscuring the relief of the vertical pore pits in some cases. All scale bars are 10 μm. Also available online as an "enhanced" high-resolution figure in the HTML version.

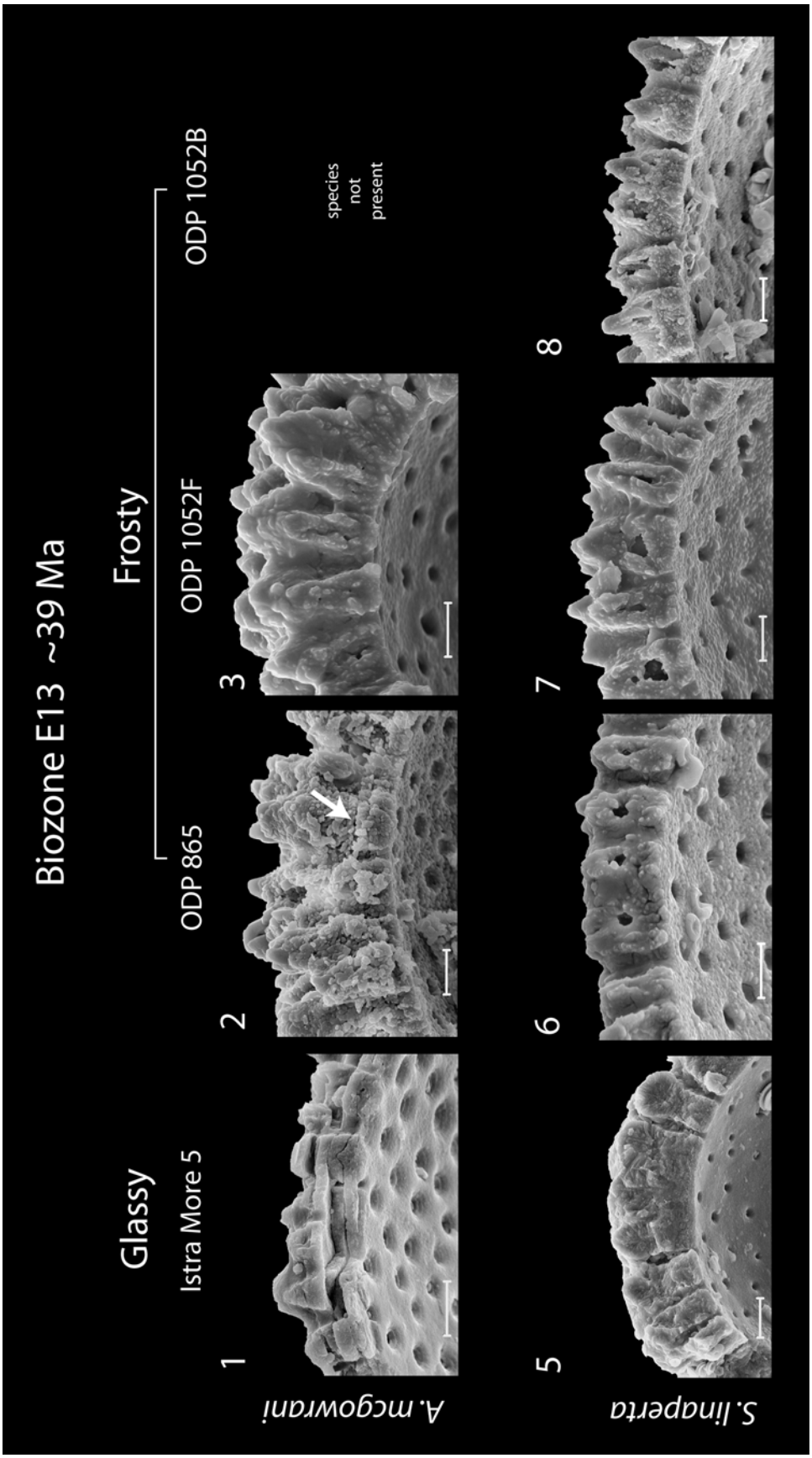
Biozone E13 ~39 Ma
Glassy
Istra More 5
Frosty
ODP 865
ODP 1052F
ODP 1052B
species not present
A. mcgowrani
S. linaperta
1
2
3
5
6
7
8

Figure 8

offset toward higher values for frosty specimens from typical pelagic samples is incorporation of diagenetic calcite onto or within the foraminiferal test at the low temperatures of the seafloor. These $\delta^{18}O$ offsets (~2.0‰ (biozone E9) and ~1.2‰ (biozone E13)) between diagenetically altered planktic foraminifera and glassy foraminifera are consistent with the predictions of numerical modeling experiments [*Schrag et al.*, 1995; *Schrag*, 1999].

[23] It is notable that we find no significant differences between glassy and frosty foraminiferal calcite for either the absolute $\delta^{13}C$ values of individual species or the range of $\delta^{13}C$ values across whole assemblages (Figures 9 and 10). It therefore appears that $\delta^{13}C$ signals in foraminiferal calcite are altered to a lesser degree during diagenesis compared to $\delta^{18}O$.

6.2. Mg/Ca Data

[24] $\delta^{13}C$ signals in carbonates are generally thought to be less susceptible to diagenetic alteration [*Scholle and Arthur*, 1980; *Veizer et al.*, 1999], because of the buffering effect on pore fluids of the large sedimentary carbonate reservoir. Indeed, this supposition agrees with our data that indicate no significant differences between $\delta^{13}C$ values of glassy and frosty foraminiferal assemblages. It is therefore informative to plot both $\delta^{18}O$ and Mg/Ca against $\delta^{13}C$ in order to examine contrasting responses to diagenetic alteration in the two former proxies. The relationship between planktic foraminiferal Mg/Ca and $\delta^{13}C$ is shown for all eight samples within biozones E9 and E13 (Figures 9 and 10, respectively).

[25] The most notable feature of the planktic foraminiferal Mg/Ca data is that, with one exception (*Globigerinatheka* spp.), Mg/Ca in exceptionally well preserved glassy material from hemipelagic sites TDP 2 (Figure 9b) and Istra More 5 (Figure 10b) yield similar relative depth rankings to those inferred from $\delta^{18}O$ data (Figures 9a and 10a). This suggests that both the Mg/Ca and $\delta^{18}O$ signatures in these glassy planktic foraminifera are unaltered and that Mg/Ca ratios in Eocene planktic foraminiferal calcite do record paleotemperature information.

[26] A second feature of the data is that for some typical pelagic samples a disagreement exists between relative depth orderings of frosty assemblages inferred from $\delta^{18}O$ and Mg/Ca data. For example, at DSDP Site 523 the relative species ordering based on Mg/Ca (Figure 9d) is quite different from that inferred from $\delta^{18}O$ (Figure 9c). In fact, at ODP Site 865 in biozone E9, the relative species ordering based on Mg/Ca (Figure 9h) is almost the reverse of that inferred from $\delta^{18}O$ (Figure 9g). In some frosty, diagenetically altered samples from typical pelagic sites, Mg/Ca and $\delta^{18}O$ in certain planktic foraminiferal species therefore appear to display different geochemical behavior during diagenetic alteration. This finding suggests that paleotemperature interpretations of Mg/Ca in frosty planktic foraminiferal calcite are not straightforward.

[27] The third feature of the planktic foraminiferal Mg/Ca data is that, in general, species with frosty taphonomies register marginally higher Mg/Ca than corresponding species with glassy taphonomies (Figures 9 and 10). However, this intraspecies Mg/Ca offset (frosty versus glassy) is more variable than the intraspecies offsets seen in $\delta^{18}O$. Considering the visual (Figures 1 and 3–8) and $\delta^{18}O$ (Figures 9 and 10) evidence for diagenetic alteration, one explanation for higher Mg/Ca values in frosty foraminifera is the presence of inorganic calcite. However, laboratory experiments designed to calculate D_{Mg} for inorganic calcite predict that inorganic calcite should contain much more Mg^{2+} than primary biogenic foraminiferal calcite (over an order of magnitude more Mg^{2+} in inorganic calcite, Table 2). Therefore the presence of even a small volume of secondary inorganic calcite in diagenetically altered foraminifera would be expected to elevate mean foraminiferal test Mg/Ca to values greatly exceeding those from contemporaneous unaltered glassy foraminifera. Yet we observe only a marginal increase in Mg/Ca of diagenetically altered foraminifera. This apparent inconsistency can be explained in a number of ways:

Figure 8. Detailed images of the wall cross sections of two planktic foraminiferal species (*A. mcgowrani*, a mixed layer dweller, and *S. linaperta*, a deeper thermocline dweller) from biozone E13. Foraminifera were taken from the same samples as those used for Figures 4 and 6. The broken glassy tests from Istra More 5 display the microgranular texture that is characteristic of biogenic calcite in Recent planktic foraminifera. Micron-scale diagenetic alteration in the broken frosty tests from "typical pelagic" DSDP and ODP drill sites is evident, even obscuring the relief of the vertical pore pits in some cases. All scale bars are 10 μm. Also available online as an "enhanced" high-resolution figure in the HTML version.

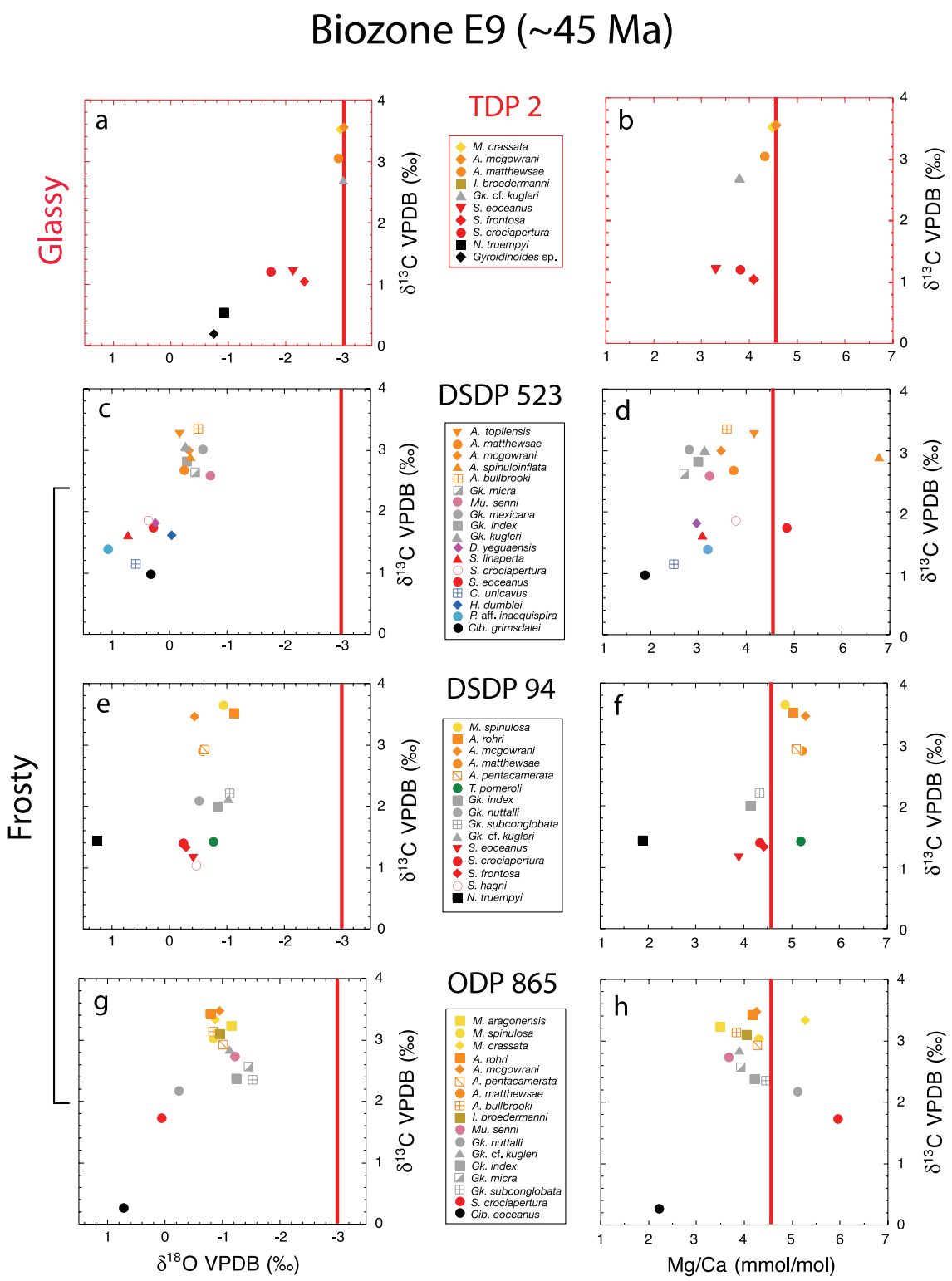

Figure 9. Multispecies stable isotope ($\delta^{18}O$ versus $\delta^{13}C$) and trace element (Mg/Ca versus $\delta^{13}C$) plots for the samples from hemipelagic drill site TDP 2 (hosting glassy foraminifera) and three other "typical pelagic" drill sites, DSDP 94, DSDP 523, and ODP 865 (hosting frosty foraminifera), from planktic foraminiferal biozone E9. Vertical red lines indicate the lowest $\delta^{18}O$ and highest Mg/Ca values recorded in the sample with glassy foraminifera (red framed plots, TDP 2). Planktic foraminiferal species from "typical pelagic" samples (black framed plots) consistently record higher $\delta^{18}O$ and frequently slightly higher Mg/Ca than given species from the hemipelagic sample. Black symbols are data from benthic foraminifera.

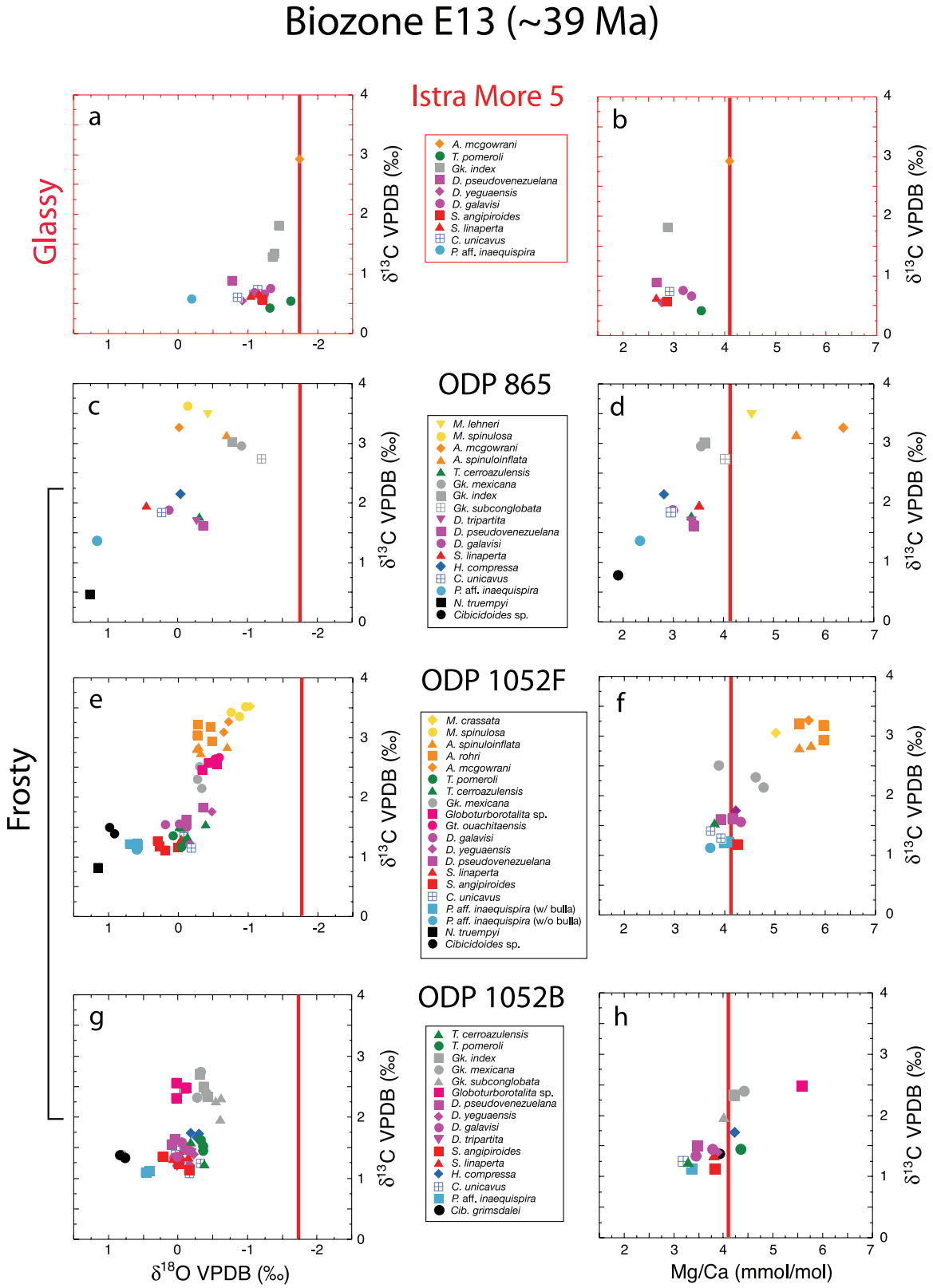
Biozone E13 (~39 Ma)
Glassy
Frosty
Istra More 5
A. mcgowrani
T. pomeroli
Gk. index
D. pseudovenezuelana
D. yeguaensis
D. galavisi
S. angipiroides
S. linaperta
C. unicavus
P. aff. inaequispira
ODP 865
M. lehneri
M. spinulosa
A. mcgowrani
A. spinuloinflata
T. cerroazulensis
Gk. mexicana
Gk. index
Gk. subconglobata
D. tripartita
D. pseudovenezuelana
D. galavisi
S. linaperta
H. compressa
C. unicavus
P. aff. inaequispira
N. truempyi
Cibicidoides sp.
ODP 1052F
M. crassata
M. spinulosa
A. spinuloinflata
A. rohri
A. mcgowrani
T. pomeroli
T. cerroazulensis
Gk. mexicana
Globoturborotalita sp.
Gt. ouachitaensis
D. galavisi
D. yeguaensis
D. pseudovenezuelana
S. linaperta
S. angipiroides
C. unicavus
P. aff. inaequispira (w/ bulla)
P. aff. inaequispira (w/o bulla)
N. truempyi
Cibicidoides sp.
ODP 1052B
T. cerroazulensis
T. pomeroli
Gk. index
Gk. mexicana
Gk. subconglobata
Globoturborotalita sp.
D. pseudovenezuelana
D. yeguaensis
D. galavisi
D. tripartita
S. angipiroides
S. linaperta
H. compressa
C. unicavus
P. aff. inaequispira
Cib. grimsdalei
δ13C VPDB (‰)
δ18O VPDB (‰)
Mg/Ca (mmol/mol)

Figure 10

Table 2. Comparison of D_{Mg} Calculated for Inorganic Calcite and for Planktic Foraminiferal Calcite[a]

	Inorganic Calcite			
	Method	Study	Precipitation Temp., °C	D_{Mg}
Laboratory experiments	Direct precipitation of calcite	*Winland* [1969]	20.0	0.01900
	Replacement of aragonite to calcite	*Katz* [1973]	25.0	0.05730
	Direct precipitation of calcite overgrowths on calcite seeds from seawater	*Mucci and Morse* [1983]	25.0	0.01200 to 0.01890
	Inorganic calcite overgrowths precipitated from seawater	*Mucci* [1987]	5.0 25.0 40.0	0.01210 0.01720 0.02710
	Direct precipitation of calcite overgrowths on calcite seeds from seawater	*Oomori et al.* [1987]	25.0	0.01900
Deep ocean sedimentary sections	Analyses of diagenetic carbonates and assoc. pore waters in deep ocean drill sites	*Baker et al.* [1982]	~5.0	0.00081
	Planktic Foraminiferal Calcite			
	Method	Study	Calcification Temp., °C	D_{Mg}
Core tops	*G. ruber* Mg/Ca calcified in seawater	*Lea et al.* [2000]	24.5 24.5 26.2 26.2	0.00050 0.00052 0.00058 0.00061
	G. ruber Mg/Ca calcified in seawater	*Dekens et al.* [2002]	23.5 26.2	0.00057 0.00048
Sediment traps	*G. ruber* Mg/Ca calcified in seawater	*Anand et al.* [2003]	25.0	0.00073 to 0.00085

[a] See equation (1) for definition of D_{Mg}. Calculations of D_{Mg} for Recent (core tops and sediment traps) planktic foraminifera are based on calcite secretion at temperatures similar to those used in the laboratory experiments for inorganic calcite (i.e., ~25°C). D_{Mg} calculated here for Recent planktic foraminifera use a modern seawater Mg/Ca molar ratio of 5.1.

[28] 1. Primary Mg/Ca values in planktic foraminiferal calcite are robust, even to significant diagenetic alteration, and the slightly higher Mg/Ca values seen in frosty material are symptomatic of higher paleotemperatures at the typical pelagic sites.

[29] 2. Laboratory-based calculations of a relatively high D_{Mg} for inorganic calcite are valid for deep sea sedimentary sections, but the frosty foraminiferal calcite is not as significantly altered as the SEM evidence and $\delta^{18}O$ data suggest.

[30] 3. $\delta^{18}O$ and Mg/Ca respond differently to the "openness" of the diagenetic system in which inorganic calcite precipitation occurs, or to the mode of diagenetic alteration (neomorphism, infilling, overgrowths).

[31] 4. SEM and $\delta^{18}O$ evidence in favor of extensive alteration of frosty foraminiferal calcite is

Figure 10. Multispecies stable isotope ($\delta^{18}O$ versus $\delta^{13}C$) and trace element (Mg/Ca versus $\delta^{13}C$) plots for the samples from hemipelagic drill site Istra More 5 (hosting glassy foraminifera) and three other "typical pelagic" drill sites, ODP 865, ODP 1052F, and ODP 1052B (hosting frosty foraminifera), from planktic foraminiferal biozone E13. Vertical red lines indicate the lowest $\delta^{18}O$ and highest Mg/Ca values recorded by planktic foraminifera in the sample with glassy foraminifera (red framed plots, Istra More 5). Planktic foraminiferal species from "typical pelagic" samples (black framed plots) consistently record higher $\delta^{18}O$ and frequently slightly higher Mg/Ca than given species from the hemipelagic sample. Black symbols are data from benthic foraminifera.

valid, but D_{Mg} for inorganic calcite in deep sea sedimentary sections is significantly lower than suggested by laboratory experiments (and much closer to that estimated by *Baker et al.* [1982], based on chemical analyses of diagenetic carbonates and their associated pore waters in deep ocean drill sites; Table 2).

[32] Explanation 1 is considered extremely unlikely, given the wide geographical distribution of the typical pelagic sites (Figure 2b), and the sensitivity of planktic foraminiferal Mg/Ca to diagenetic alteration documented for the Pleistocene to Recent [*Brown and Elderfield*, 1996; *Lea et al.*, 2000; *Rosenthal et al.*, 2000; *Dekens et al.*, 2002]. Explanation 2 requires that the total mass of inorganic calcite on frosty tests must be extremely small in comparison to the total mass of unaltered primary biogenic calcite comprising the test (despite being inconsistent with the visual evidence for pervasive alteration throughout the test, section 5.3, Figures 7 and 8). Thus mean test Mg/Ca is only slightly increased by the addition of relatively minor amounts of secondary inorganic calcite. However, if this is correct, the significantly higher $\delta^{18}O$ values in frosty calcite imply that we do not understand the process of calcite $\delta^{18}O$ alteration during diagenesis. Explanations 3 and 4 are our favored interpretations. Explanation 3 may be at least partly valid, but unfortunately there are at present no data with which to test this hypothesis. With regard to explanation 4, the only geological study to estimate D_{Mg} in a deep sea sedimentary section based on geochemical data arrives at a value for D_{Mg} that is more than one order of magnitude lower (~0.0008 at ~5°C [*Baker et al.*, 1982]) than that derived in laboratory experiments (e.g., ~0.0121 at ~5°C [*Mucci*, 1987]) (see Table 2). Addition of even significant amounts of inorganic calcite with a relatively low D_{Mg} [e.g., *Baker et al.*, 1982] would thereby cause only a relatively small increase in Mg/Ca of the diagnetically altered foraminiferal test.

7. Impact of Diagenesis on Multiproxy SST Estimates

[33] Paleotemperatures are calculated using the multispecies planktic foraminiferal Mg/Ca and $\delta^{18}O$ data from the various sites on the basis of different assumptions for Mg/Ca and $\delta^{18}O$ compositions of middle Eocene seawater (Mg/Ca_w and $\delta^{18}O_w$). These calculated paleotemperatures provide a semi-quantitative estimation of the potential bias introduced into paleoclimatic reconstructions by diagenetic alteration. Figure 11 shows Mg/Ca-derived (red symbols) and $\delta^{18}O$-derived (blue symbols) paleotemperatures for all analyzed species within all four samples in each biozone. Paleotemperatures from the hemipelagic sites, hosting glassy planktic foraminifera showing no obvious signs of diagenetic alteration, should provide reliable paleotemperature estimates for biozones E9 and E13, against which we compare paleotemperature estimates from the other sites hosting frosty foraminiferal calcite.

[34] Surface dwelling planktic foraminifera from the glassy hemipelagic material in biozone E9 (TDP 2; ~45 Ma) yield maximum Mg/Ca-derived SSTs of 30°C (assuming modern Mg/Ca_w of 5.1 mol/mol, vertical red line, Figure 11). Accounting for secular change in Mg/Ca_w since the middle Eocene (Mg/Ca_w assumptions of 4.1 [*Lear et al.*, 2002], 3.1 (mean ratio from fluid inclusions [*Zimmermann*, 2000; *Lowenstein et al.*, 2001]), and 1.6 mol/mol [*Hardie*, 1996]) yields even warmer Mg/Ca-derived SSTs of 32°C, 35°C, and 43°C, respectively. All these SST estimates are significantly higher than modern (for the same latitude), and support the concept of a "greenhouse"-driven climate during the early middle Eocene. However, SSTs of 43°C (assuming Mg/Ca_w = 1.6 mol/mol [*Hardie*, 1996]) are unrealistically warm (compared to existing middle Eocene data), and instead imply that early middle Eocene Mg/Ca_w likely lay within the range of 5.1 to 3.1 mol/mol.

[35] For biozone E9, $\delta^{18}O$-derived SSTs using an assumption for middle Eocene $\delta^{18}O_w$ of −1.0‰ (approximating an ice-free planet [*Lear et al.*, 2000; *Zachos et al.*, 2001]) yields SSTs that are cooler (by at least 5°C) than all Mg/Ca-derived estimates. Even with a higher $\delta^{18}O_w$ of −0.5‰ (although probably an overestimate [*Lear et al.*, 2000; *Zachos et al.*, 2001]; vertical dashed blue line, Figure 11), SSTs still do not quite approach those of even the coolest Mg/Ca-derived estimates. For late middle Eocene biozone E13 (~39 Ma) Mg/Ca-derived SSTs for the hemipelagic site hosting glassy foraminifera (Istra More 5) are slightly cooler (reaching 27°C with modern Mg/Ca_w; red line, Figure 11) compared to those from the hemipelagic site (TDP 2) from early middle Eocene biozone E9. Again, $\delta^{18}O$-inferred SSTs yield much cooler paleotemperatures, with SSTs only reaching 21°C assuming a $\delta^{18}O_w$ of −0.5‰ (dashed blue line). In comparing $\delta^{18}O$- and Mg/Ca-derived paleotemperatures it is premature to attempt to estimate $\delta^{18}O_w$ at either hemipelagic site because the mul-

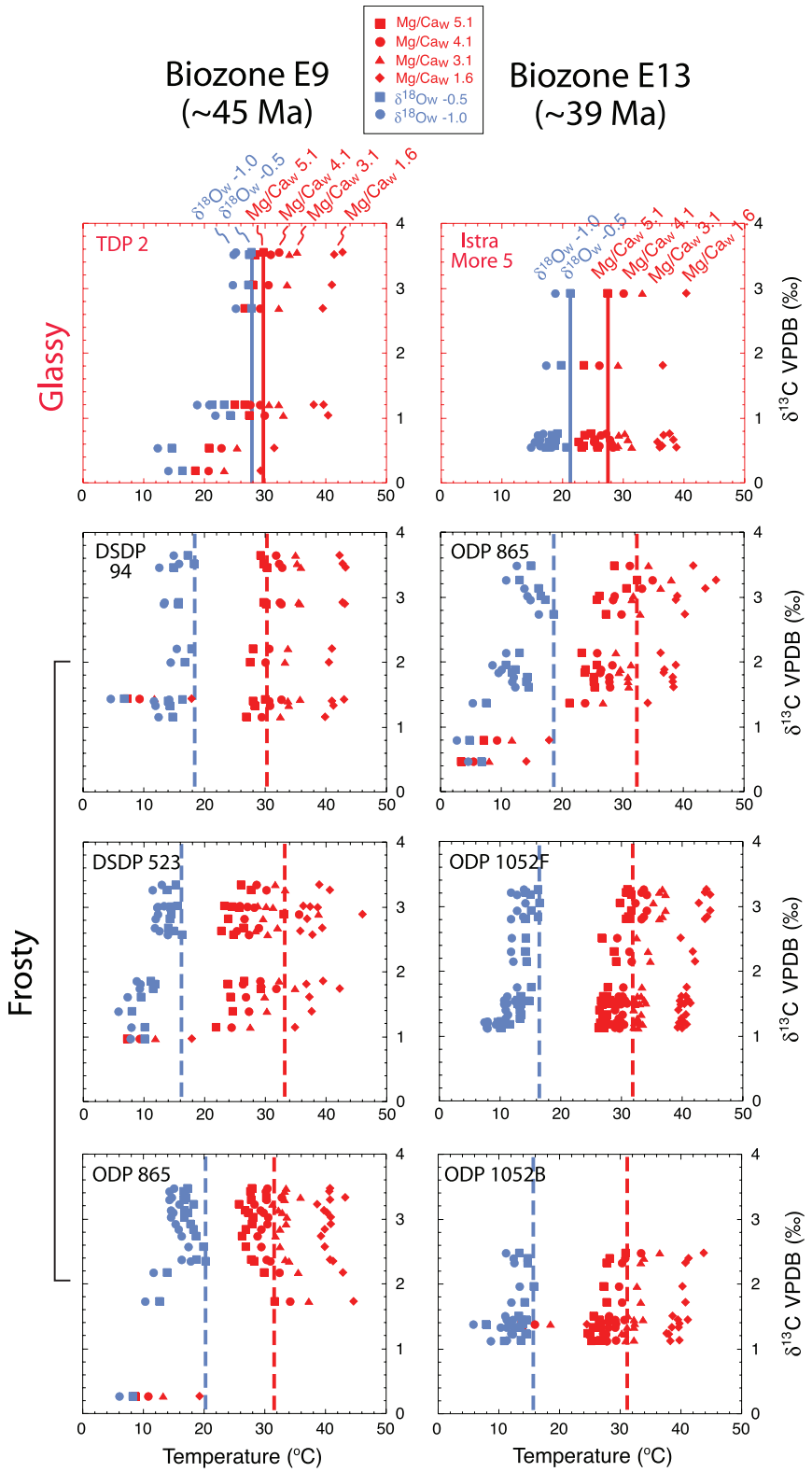
Biozone E9
(~45 Ma)
Biozone E13
(~39 Ma)
Mg/Caw 5.1
Mg/Caw 4.1
Mg/Caw 3.1
Mg/Caw 1.6
δ18Ow -0.5
δ18Ow -1.0
Glassy
Frosty
TDP 2
Istra
More 5
DSDP
94
ODP 865
DSDP 523
ODP 1052F
ODP 865
ODP 1052B
δ13C VPDB (‰)
Temperature (°C)

Figure 11

tispecies data for both biozones are from single samples (i.e., comprising 6 to 14 individual tests) and at present there are few constraints on the magnitude of planktic foraminiferal inter-species "vital effects" in Mg/Ca.

[36] Regardless of the true SSTs for either of the hemipelagic sites (TDP 2 and Istra More 5), the three typical pelagic sites in each biozone all reveal similar patterns in their relative paleotemperature estimates. δ^{18}O-derived SSTs for typical pelagic sites are approximately 8 to 12°C (E9) and 4 to 6°C (E13) cooler than those calculated for the hemipelagic sites (Figure 11). Inferred tropical to subtropical SSTs of 16 to 20°C for these typical pelagic sites are cool for the middle Eocene and, when considered in light of the SEM imaging evidence for diagenetic alteration (Figures 1 and 3–8), past practice of using frosty, diagenetically altered material such as this is the likely explanation for the "cool tropic paradox." Conversely, the marginally higher Mg/Ca-derived paleotemperatures for frosty calcite (compared to glassy hemipelagic calcite) are difficult to interpret in terms of substantial addition of inorganic calcite with a relatively high D_{Mg}. This discrepancy may be resolved by invoking a much lower D_{Mg} for inorganic calcite, one that is more in line with the estimate of *Baker et al.* [1982] (Table 2).

8. Toward Quantifying the Extent of Foraminiferal Diagenetic Alteration

[37] Greater understanding of the respective geochemical compositions of inorganic and biogenic calcite is required if we are to gain more quantitative estimates of the relative contributions of each to the diagenetically altered foraminiferal test. However, few data are available on the geochemical composition of inorganic calcite in pelagic sedimentary sequences. This situation is partly a result of the often very small size (on the order of microns) of secondary inorganic calcite crystals, frequently growing on or within the fossil tests or plates of calcifying organisms which serve as crystallization nuclei. Here we calculate the down core Mg/Ca composition of secondary inorganic calcite at Site 1052 using pore fluid [Mg^{2+}] and [Ca^{2+}] data measured at this site [*Norris et al.*, 1998] and by making assumptions concerning the factors influencing the Mg/Ca composition of inorganic calcite. The resultant calculations produce a range of estimates for the Mg/Ca composition of secondary inorganic calcite that have implications for the extent of diagenetic geochemical alteration of planktic foraminifera hosted in this sedimentary sequence.

[38] Rearranging equation (1), the Mg/Ca composition of inorganic calcite is given by

$$(Mg/Ca)_s = D_{Mg} \cdot (Mg/Ca)_{fl}. \quad (2)$$

We calculate down core values of inorganic calcite $(Mg/Ca)_s$ at Site 1052 (shown in Figure 12), using the two contrasting estimates of D_{Mg} from Table 2 [*Mucci*, 1987; *Baker et al.*, 1982]. Using in situ pore fluid Mg/Ca data from ODP Site 1052 to represent $(Mg/Ca)_{fl}$ is an oversimplification because it assumes that crystal growth of inorganic calcite occurred from pore fluids with a similar composition to the modern pore fluid profile [e.g., *Rudnicki et al.*, 2001]. However, because the pore fluid gradients are so gentle, even if most crystal growth occurred at the seafloor or during very shallow burial, the differential effect on $(Mg/Ca)_s$ will be small.

[39] Figure 12 shows the relative influence on calculated inorganic $(Mg/Ca)_s$ of a range of variables including values of D_{Mg}, pore fluid $(Mg/Ca)_{fl}$, geothermal gradients, bottom water temperatures (BWTs) and variations in seawater Mg/Ca. The figure shows that values of D_{Mg} are paramount in determining the values of inorganic $(Mg/Ca)_s$ and

Figure 11. Multispecies Mg/Ca-derived and δ^{18}O-derived paleotemperature estimates for each drill site using various assumptions for Mg/Ca and δ^{18}O composition of mean global middle Eocene seawater. Vertical lines indicate highest Mg/Ca-derived (red; assuming modern seawater Mg/Ca) and δ^{18}O-derived (blue; assuming a $\delta^{18}O_w$ of −0.5‰) paleotemperatures recorded by planktic foraminifera with glassy (solid lines) and frosty (dashed lines) taphonomies. Highest paleotemperatures for the foraminiferal assemblages are used to infer SST. Mg/Ca-derived paleotemperatures are calculated using the Mg/Ca-temperature equation for *G. sacculifer* calibrated from sediment trap time series [*Anand et al.*, 2003]. δ^{18}O-derived paleotemperatures are calculated using the δ^{18}O paleotemperature equation for asymbiotic planktic foraminifera from *Bemis et al.* [1998]. The scenarios for middle Eocene Mg/Ca_w are molar ratios of 4.1 [*Lear et al.*, 2002], 3.1 (mean ratio from fluid inclusions [*Zimmermann*, 2000; *Lowenstein et al.*, 2001]), and 1.6 [*Hardie*, 1996] at ~49 Ma. Given species with frosty taphonomies from "typical pelagic" samples (black framed plots) record marginally higher Mg/Ca-derived paleotemperatures for given seawater Mg/Ca scenarios compared to hemipelagic samples (red framed plots). Given species from "typical pelagic" samples also record consistently lower δ^{18}O-derived paleotemperatures.

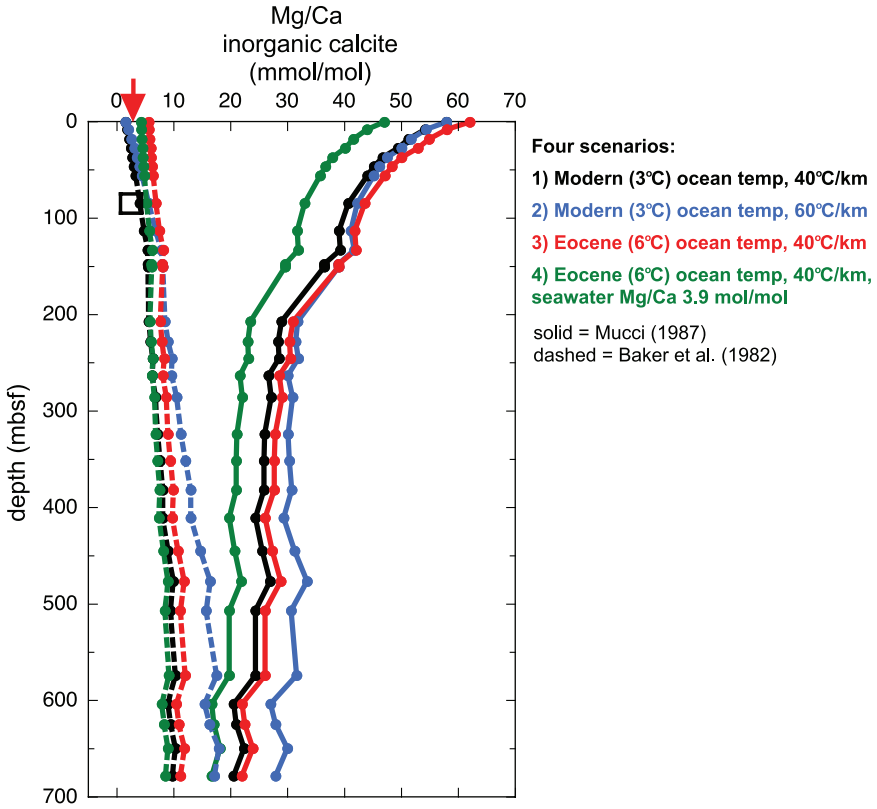

Figure 12. Mg/Ca of inorganic calcite calculated down core at ODP Site 1052 using pore fluid [Ca^{2+}] and [Mg^{2+}] data measured at this site [*Norris et al.*, 1998]. Inorganic calcite Mg/Ca is calculated using two different values for D_{Mg}: a laboratory-based value [*Mucci*, 1987] (solid lines) and one calculated from a deep ocean sedimentary section [*Baker et al.*, 1982] (dashed lines). An exponential fit was applied to the *Mucci* [1987]D_{Mg}-temperature data (comprising estimates of D_{Mg} at 5, 25, and 40°C). Because the *Baker et al.* [1982] data comprise only a single estimate for D_{Mg} (at 5°C), the same exponential relationship seen in the *Mucci* [1987] data was applied to the *Baker et al.* [1982] data. The decrease in inorganic calcite Mg/Ca with depth seen for the *Mucci* [1987] D_{Mg} curves reflects the net dominance of decreasing pore fluid Mg/Ca over the geothermal temperature increase. Conversely, the slight increase in inorganic calcite Mg/Ca with depth seen for the *Baker et al.* [1982]D_{Mg} curves arises because the absolute value for D_{Mg} used in their construction is so low (see Table 2). Consequently, the temperature-related proportional increase in D_{Mg} with depth (driven by the geothermal gradient) is greater than the proportional decrease in pore fluid Mg/Ca (itself a function of the gentle pore fluid gradients at Site 1052). Four scenarios are used to calculate Mg/Ca for inorganic calcite: (1) Modern BWT (3°C), geothermal gradient of 40°C/km. (2) Modern BWT (3°C), geothermal gradient of 60°C/km. (3) Middle Eocene BWT (6°C), geothermal gradient of 40°C/km. (4) Middle Eocene BWT (6°C), geothermal gradient of 40°C/km, and middle Eocene seawater Mg/Ca molar ratio of 3.9. Pore fluid Mg/Ca values at the seafloor (0 mbsf) are assumed to equal the modern seawater Mg/Ca molar ratio of 5.1 in all scenarios except 4. Geothermal gradient estimates taken from *Zwart et al.* [1996] and *Rao et al.* [2001]. Middle Eocene mean BWT calculated from Site 1052 benthic foraminiferal $\delta^{18}O$ data of *Sexton* [2005]. Middle Eocene seawater Mg/Ca molar ratio taken from *Wilkinson and Algeo* [1989]. Black box indicates range of Mg/Ca values for frosty planktic foraminiferal calcite from "typical pelagic" drill site ODP 1052 (Figures 10f and 10h). Red arrow indicates approximate Mg/Ca values for glassy planktic foraminiferal calcite from hemipelagic drill sites TDP 2 and Istra More 5. Calculations of inorganic calcite Mg/Ca using the two different values for D_{Mg} imply very different diagenetic histories for Site 1052 foraminifera, as shown by the similarity of calculated inorganic Mg/Ca (using the *Baker et al.* [1982] D_{Mg}) to measured frosty foraminiferal Mg/Ca (black box).

the rate and even direction of change of inorganic $(Mg/Ca)_s$ with depth. The calculated estimates of inorganic $(Mg/Ca)_s$ for Site 1052 (Figure 12) can be compared with Mg/Ca ratios of planktic foraminiferal calcite from the same site (Figures 10f and 10h). In this way, we can test the assumption of significant addition of inorganic calcite to planktic foraminifera based on the SEM imaging and $\delta^{18}O$ data. Although we cannot gauge precisely when foraminifera at Site 1052 may have under-

gone diagenetic alteration (numerical modeling suggests at an early stage during shallow burial, with minimal influence of pore fluid chemistry [*Rudnicki et al.*, 2001]), the various influences on inorganic calcite Mg/Ca that have the potential to exhibit secular variation (e.g., pore fluid $(Mg/Ca)_{fl}$, seawater Mg/Ca, BWT) are all subordinate factors compared to the dominating influence of D_{Mg} (Figure 12).

[40] The combined range of planktic foraminiferal Mg/Ca values from the two frosty samples from Site 1052 (Figures 10f and 10h) is represented by the black box in Figure 12. There are three possible interpretations of the relationship between calculated inorganic Mg/Ca and measured planktic foraminiferal Mg/Ca values (black box) shown in this figure. First, at the burial depth of the two samples (86 and 97 mbsf), values of inorganic $(Mg/Ca)_s$ calculated using the *Mucci* [1987] D_{Mg} are approximately an order of magnitude greater than the measured Mg/Ca for Site 1052 planktic foraminifera (black box, Figure 12). Furthermore, in the context of this large difference between calculated inorganic calcite Mg/Ca (using *Mucci* [1987] D_{Mg}) and foraminiferal Mg/Ca, Mg/Ca values of frosty planktic foraminifera from Site 1052 lie relatively close to those of contemporaneous glassy planktic foraminifera from Istra More 5 (red arrow, Figure 12). From these observations it would appear that the proportion of inorganic calcite incorporated within Site 1052 planktic foraminiferal tests must be minimal. However, this is inconsistent with SEM and $\delta^{18}O$ evidence for significant diagenetic alteration of Site 1052 planktic foraminiferal calcite.

[41] A second possible interpretation is that the laboratory-based D_{Mg} values for inorganic calcite [e.g., *Mucci*, 1987] are valid and significant diagenetic alteration has occurred, but that diagenetic alteration occurred in a relatively "closed" system where dissolution of primary biogenic calcite (i.e., foraminifera, nannofossils) directly supplied a large proportion of the Mg^{2+} and Ca^{2+} cations that were subsequently re-incorporated back onto the foraminiferal test in inorganic form. Because biogenic calcite typically has a Mg/Ca ratio over three orders of magnitude lower than that of modern seawater, a foraminiferal test that is diagenetically altered in a relatively closed system would have a bulk Mg/Ca value that is much closer to the original Mg/Ca of the biogenic source material (notwithstanding the temperature gradient between the upper ocean and the seafloor that would cause a small decrease in values of inorganic $(Mg/Ca)_s$). This interpretation is based on the fact that the pore water $(Mg/Ca)_{fl}$ values from Site 1052 possibly over-estimate the specific $(Mg/Ca)_{fl}$ values at the micro-sites where diagenetic alteration occurs. Pore water samples represent an average value over a relatively large area (e.g., pore water data are derived from ~135 cc sediment volume), but diagenetic alteration of foraminiferal calcite probably occurs within micro-systems in the pore spaces occupied by individual foraminifera. Release of Ca^{2+} through dissolution of biogenic calcite (i.e., foraminifera, nannofossils) could thereby drive $(Mg/Ca)_{fl}$ in these specific microenvironments to values lower than those predicted by large volume pore water samples.

[42] Because inorganic $(Mg/Ca)_s$ calculated using the *Baker et al.* [1982] D_{Mg} yields Mg/Ca values only slightly higher than those for measured frosty planktic foraminiferal Mg/Ca (black box, Figure 12), a third interpretation is that planktic foraminifera from Site 1052 incorporate a significant amount of inorganic calcite within their tests. This is compatible with SEM imaging and $\delta^{18}O$ evidence for significant diagenetic alteration of planktic foraminiferal calcite at Site 1052.

9. Conclusions

[43] Detailed SEM images presented here reveal that the nature of planktic foraminiferal diagenetic alteration appears to be micron-scale inorganic calcite overgrowths covering the surface, and growing on the interior walls, of the foraminiferal test. In addition, images of wall cross sections are suggestive of neomorphism and/or dissolution. These diagenetic features are extensive in foraminiferal tests from typical pelagic settings (which appear "frosty" when viewed under reflected light) and absent in tests from hemipelagic clay-rich settings (which appear "glassy" under reflected light). Our visual observations suggest that diagenetic alteration in the frosty foraminiferal assemblages examined here is pervasive, although our geochemical data are equivocal in this regard.

[44] Despite the influence of micron-scale diagenetic alteration significantly lowering $\delta^{18}O$-derived paleotemperatures in frosty foraminiferal tests from typical pelagic samples, the relatively consistent intraspecies $\delta^{18}O$ (and $\delta^{13}C$) offsets presented here between given species with frosty versus glassy taphonomies suggest that relative $\delta^{18}O$ (and $\delta^{13}C$) offsets between species within an assemblage may

be generally preserved following diagenetic alteration. Frosty planktic foraminiferal calcite therefore remains valuable for generating relatively short (approximately $\leq$1 Myr) time series concerned with temporal trends and rates of change in paleoceanographic variables.

[45] A consistent discrepancy has been documented between the relative extents of $\delta^{18}O$ and Mg/Ca alteration in given species suffering from obvious diagenetic alteration, when compared to the same contemporaneous species exhibiting a glassy taphonomy. The relatively small influence of diagenetic alteration on foraminiferal test Mg/Ca suggests either that $\delta^{18}O$ and Mg/Ca respond differently to diagenetic alteration or that a much lower Mg^{2+} partition coefficient (compared to laboratory-based estimates) is more appropriate for inorganic calcite precipitating in deep sea sedimentary sections (in accordance with the findings of *Baker et al.* [1982]).

Acknowledgments

[46] We thank Matt Cooper, Mike Bolshaw, and Richard Pearce for laboratory assistance and members of the Paleogene Planktic Foraminifera Working Group for discussions on taxonomy and paleoecology. We also thank Dick Kroon, Carrie Lear, and John Murray for insightful discussions and Rachael James and James Zachos for thorough and very helpful reviews. This research used samples and data provided by the Ocean Drilling Program (ODP). ODP (now IODP) is sponsored by the U.S. National Science Foundation (NSF) and participating countries under management of Joint Oceanographic Institutions (JOI), Inc. Financial support for this research was provided by Natural Environment Research Council studentship GT04/97/ES/46 (to P.F.S.) and a UK ODP (NERC) grant (to P.A.W.).

References

Allison, N., and W. E. N. Austin (2003), The potential of ion microprobe analysis in detecting geochemical variations across individual foraminifera tests, *Geochem. Geophys. Geosyst.*, *4*(2), 8403, doi:10.1029/2002GC000430.

Anand, P., H. Elderfield, and M. H. Conte (2003), Calibration of Mg/Ca thermometry in planktonic foraminifera from a sediment trap time series, *Paleoceanography*, *18*(2), 1050, doi:10.1029/2002PA000846.

Baker, P. A., J. M. Gieskes, and H. Elderfield (1982), Diagenesis of carbonates in deep-sea Sediments—Evidence from Sr/Ca ratios and interstitial dissolved Sr^{2+} data, *J. Sediment. Petrol.*, *52*, 71–82.

Barker, S., M. Greaves, and H. Elderfield (2003), A study of cleaning procedures used for foraminiferal Mg/Ca paleothermometry, *Geochem. Geophys. Geosyst.*, *4*(9), 8407, doi:10.1029/2003GC000559.

Barrera, E. (1994), Global environmental changes preceding the Cretaceous-Tertiary boundary: Early–late Maastrichtian transition, *Geology*, *22*, 877–880.

Barrera, E., and B. T. Huber (1991), Paleogene and early Neogene oceanography of the southern Indian Ocean: Leg 119 foraminifer stable isotope results, *Proc. Ocean Drill. Program Sci. Results*, *119*, 693–717.

Barron, E. J., W. H. Peterson, D. Pollard, and S. Thompson (1993), Past climate and the role of ocean heat transport: Model simulations for the Cretaceous, *Paleoceanography*, *8*, 785–798.

Bemis, B. E., H. J. Spero, J. Bijma, and D. W. Lea (1998), Reevaluation of the oxygen isotopic composition of planktonic foraminifera: Experimental results and revised paleotemperature equations, *Paleoceanography*, *13*, 150–160.

Berggren, W., D. Kent, and C. Swisher, III, (1995), A revised Cenozoic geochronology and chronostratigraphy, in *Geochronology Time Scales and Global Stratigraphic Correlation*, edited by W. Berggren, pp. 129–212, Soc. for Sediment. Geol., Tulsa, Okla.

Berggren, W. A., and P. N. Pearson (2005), A revised tropical to subtropical Paleogene planktonic foraminiferal zonation, *J. Foraminiferal Res.*, *35*, 279–298.

Berner, R. A. (1994), GEOCARB II: A revised model of atmospheric CO_2 over Phanerozoic time, *Am. J. Sci.*, *294*, 56–91.

Berner, R. A., and Z. Kothavala (2001), GEOCARB III: A revised model of atmospheric CO_2 over Phanerozoic time, *Am. J. Sci.*, *301*, 182–204.

Berner, R. A., A. C. Lasaga, and R. M. Garrels (1983), The carbonate-silicate geochemical cycle and its effect on atmospheric carbon-dioxide over the past 100 million years, *Am. J. Sci.*, *283*, 641–683.

Bice, K. L., and R. D. Norris (2002), Possible atmospheric CO_2 extremes of the Middle Cretaceous (late Albian–Turonian), *Paleoceanography*, *17*(4), 1070, doi:10.1029/2002PA000778.

Boersma, A., I. Premoli Silva, and N. J. Shackleton (1987), Atlantic Eocene planktonic foraminiferal paleohydrographic indicators and stable isotope paleoceanography, *Paleoceanography*, *2*, 287–331.

Boyle, E. A., and L. D. Keigwin (1985), Comparison of Atlantic and Pacific paleochemical records for the last 215,000 years—Changes in deep ocean circulation and chemical inventories, *Earth Planet. Sci. Lett.*, *76*, 135–150.

Bralower, T. J., J. C. Zachos, E. Thomas, M. Parrow, C. K. Paull, D. C. Kelly, I. P. Silva, W. V. Sliter, and K. C. Lohmann (1995), Late Paleocene to Eocene paleoceanography of the equatorial Pacific Ocean: Stable isotopes recorded at Ocean Drilling Program Site 865, Allison Guyot, *Paleoceanography*, *10*, 841–865.

Brown, S. J., and H. Elderfield (1996), Variations in Mg/Ca and Sr/Ca ratios of planktonic foraminifera caused by postdepositional dissolution: Evidence of shallow Mg-dependent dissolution, *Paleoceanography*, *11*, 543–551.

Bush, A. B. G., and S. G. H. Philander (1997), The late Cretaceous: Simulation with a coupled atmosphere-ocean general circulation model, *Paleoceanography*, *12*, 495–516.

Coxall, H. K., P. N. Pearson, N. J. Shackleton, and M. A. Hall (2000), Hantkeninid depth adaptation: An evolving life strategy in a changing ocean, *Geology*, *28*, 87–90.

Crowley, T., and J. Zachos (2000), Comparison of zonal temperature profiles for past warm time periods, in *Warm Climates in Earth History*, edited by B. Huber, K. MacLeod and S. Wing, pp. 50–76, Cambridge Univ. Press, New York.

Crowley, T. J. (1991), Past CO_2 changes and tropical sea surface temperatures, *Paleoceanography*, *6*, 387–394.

D'Hondt, S., and M. A. Arthur (1996), Late Cretaceous oceans and the cool tropic paradox, *Science*, *271*, 1838–1841.

Dekens, P. S., D. W. Lea, D. K. Pak, and H. J. Spero (2002), Core top calibration of Mg/Ca in tropical foraminifera: Refining paleotemperature estimation, *Geochem. Geophys. Geosyst.*, *3*(4), 1022, doi:10.1029/2001GC000200.

Douglas, R. G., and S. M. Savin (1973), Oxygen and carbon isotope analyses of Cretaceous and Tertiary foraminifera from the central North Pacific, *Initial Rep. Deep Sea Drill. Proj.*, *17*, 591–607.

Douglas, R. G., and S. M. Savin (1975), Oxygen and carbon isotope analyses of Tertiary and Cretaceous microfossils from Shatsky Rise and other sites in the North Pacific Ocean, *Initial Rep. Deep Sea Drill. Proj.*, *32*, 509–520.

Eggins, S., P. De Deckker, and J. Marshall (2003), Mg/Ca variation in planktonic foraminifera tests: Implications for reconstructing palaeo-seawater temperature and habitat migration, *Earth Planet. Sci. Lett.*, *212*, 291–306.

Ekart, D. D., T. E. Cerling, I. P. Montanez, and N. J. Tabor (1999), A 400 million year carbon isotope record of pedogenic carbonate: Implications for paleoatmospheric carbon dioxide, *Am. J. Sci.*, *299*, 805–827.

Fairbanks, R. G., P. H. Wiebe, and A. W. H. Be (1980), Vertical distribution and isotopic composition of living planktonic foraminifera in the western North Atlantic, *Science*, *207*, 61–63.

Fairbanks, R. G., M. Sverdlove, R. Free, P. H. Wiebe, and A. W. H. Be (1982), Vertical distribution and isotopic fractionation of living planktonic foraminifera from the Panama Basin, *Nature*, *298*, 841–844.

Folk, R. L. (1965), Some aspects of recrystallization in ancient limestones, in *Dolomitization and Limestone Diagenesis: A Symposium*, edited by L. C. Pray and R. C. Murray, *Spec. Publ. Soc. Econ. Paleontol. Mineral.*, *13*, 14–48.

Green, D. R. H., M. J. Cooper, C. R. German, and P. A. Wilson (2003), Optimization of an inductively coupled plasma–optical emission spectrometry method for the rapid determination of high-precision Mg/Ca and Sr/Ca in foraminiferal calcite, *Geochem. Geophys. Geosyst.*, *4*(6), 8404, doi:10.1029/2002GC000488.

Hardie, L. A. (1996), Secular variation in seawater chemistry: An explanation for the coupled secular variation in the mineralogies of marine limestones and potash evaporites over the past 600 my, *Geology*, *24*, 279–283.

Hathorne, E. C., O. Alard, R. H. James, and N. W. Rogers (2003), Determination of intratest variability of trace elements in foraminifera by laser ablation inductively coupled plasma-mass spectrometry, *Geochem. Geophys. Geosyst.*, *4*(12), 8408, doi:10.1029/2003GC000539.

Haworth, M., S. P. Hesselbo, J. C. McElwain, S. A. Robinson, and J. W. Brunt (2005), Mid-Cretaceous pCO_2 based on stomata of the extinct conifer Pseudofrenelopsis (Cheirolepidiaceae), *Geology*, *33*, 749–752.

Hemleben, C., and R. K. Olsson (2006), Wall textures of Eocene planktonic foraminifera, in *Atlas of Eocene Planktonic Foraminifera*, edited by P. N. Pearson, et al., pp. 47–66, *Cushman Found. for Foraminiferal Res.*, *Spec. Publ. 41*, Allen, Lawrence, Kans.

Horrell, M. A. (1990), Energy balance constraints on $\delta^{18}O$ based paleo-sea surface temperature estimates, *Paleoceanography*, *5*, 339–348.

Huber, B. T., D. A. Hodell, and C. P. Hamilton (1995), Middle-Late Cretaceous climate of the southern high-latitudes—Stable isotopic evidence for minimal equator-to-pole thermal gradients, *Geol. Soc. Am. Bull.*, *107*, 1164–1191.

Huber, M., and L. C. Sloan (2000), Climatic responses to tropical sea surface temperature changes on a "greenhouse" Earth, *Paleoceanography*, *15*, 443–450.

Huber, M., and L. C. Sloan (2001), Heat transport, deep waters, and thermal gradients: Coupled simulation of an Eocene greenhouse climate, *Geophys. Res. Lett.*, *28*, 3481–3484.

Katz, A. (1973), The interaction of magnesium with calcite during crystal growth at 25–90°C and one atmosphere, *Geochim. Cosmochim. Acta*, *37*, 1563–1586.

Lea, D. W., D. K. Pak, and H. J. Spero (2000), Climate impact of late quaternary equatorial Pacific sea surface temperature variations, *Science*, *289*, 1719–1724.

Lear, C. H., H. Elderfield, and P. A. Wilson (2000), Cenozoic deep-sea temperatures and global ice volumes from Mg/Ca in benthic foraminiferal calcite, *Science*, *287*, 269–272.

Lear, C. H., Y. Rosenthal, and N. Slowey (2002), Benthic foraminiferal Mg/Ca-paleothermometry: A revised core-top calibration, *Geochim. Cosmochim. Acta*, *66*, 3375–3387.

Lowenstein, T. K., M. N. Timofeeff, S. T. Brennan, L. A. Hardie, and R. V. Demicco (2001), Oscillations in Phanerozoic seawater chemistry: Evidence from fluid inclusions, *Science*, *294*, 1086–1088.

Manabe, S., and K. Bryan (1985), CO_2–induced change in a coupled ocean-atmosphere model and its paleoclimatic implications, *J. Geophys. Res.*, *90*, 1689–1707.

Mucci, A. (1987), Influence of temperature on the composition of magnesian calcite overgrowths precipitated from seawater, *Geochim. Cosmochim. Acta*, *51*, 1977–1984.

Mucci, A., and J. W. Morse (1983), The incorporation of Mg^{2+} and Sr^{2+} into calcite overgrowths—Influences of growth-rate and solution composition, *Geochim. Cosmochim. Acta*, *47*, 217–233.

Norris, R. D., and P. A. Wilson (1998), Low-latitude sea-surface temperatures for the mid-Cretaceous and the evolution of planktic foraminifera, *Geology*, *26*, 823–826.

Norris, R. D., , D. Kroon, and A. Klaus (Eds.) (1998), *Proceedings of the Ocean Drilling Program, Initial Reports*, vol. 171B, Ocean Drill. Program, College Station, Tex.

Norris, R. D., K. L. Bice, E. A. Magno, and P. A. Wilson (2002), Jiggling the tropical thermostat in the Cretaceous hothouse, *Geology*, *30*, 299–302.

Oomori, T., H. Kaneshima, Y. Maezato, and Y. Kitano (1987), Distribution coefficient of Mg^{2+} ions between calcite and solution at 10–50°C, *Mar. Chem.*, *20*, 327–336.

Ortiz, J. D., A. C. Mix, W. Rugh, J. M. Watkins, and R. W. Collier (1996), Deep-dwelling planktonic foraminifera of the northeastern Pacific Ocean reveal environmental control of oxygen and carbon isotopic disequilibria, *Geochim. Cosmochim. Acta*, *60*, 4509–4523.

Pagani, M., J. C. Zachos, K. H. Freeman, B. Tipple, and S. Bohaty (2005), Marked decline in atmospheric carbon dioxide concentrations during the Paleogene, *Science*, *309*, 600–603.

Pearson, P. N. (1998), Stable isotopes and the study of evolution in planktonic foraminifera, in *Isotope Paleobiology and Paleoecology*, edited by R. D. Norris and R. M. Corfield, pp. 138–178, Paleontol. Soc., Pittsburgh, Pa.

Pearson, P. N., and M. R. Palmer (2000), Atmospheric carbon dioxide concentrations over the past 60 million years, *Nature*, *406*, 695–699.

Pearson, P. N., N. J. Shackleton, and M. A. Hall (1993), Stable isotope paleoecology of middle Eocene planktonic foraminifera and multispecies isotope stratigraphy, DSDP Site 523, South-Atlantic, *J. Foraminiferal Res.*, *23*, 123–140.

Pearson, P. N., P. W. Ditchfield, J. Singano, K. G. Harcourt-Brown, C. J. Nicholas, R. K. Olsson, N. J. Shackleton, and M. A. Hall (2001), Warm tropical sea surface temperatures in the Late Cretaceous and Eocene epochs, *Nature*, *413*, 481–487.

Pearson, P. N., R. K. Olsson, B. T. Huber, C. Hemleben, and W. A. Berggren (Eds.) (2006), *Atlas of Eocene Planktonic Foraminifera*, *Cushman Found. for Foraminiferal Res.*, *Spec. Publ. 41*, Allen, Lawrence, Kans.

Poore, R. Z., and R. K. Matthews (1984), Oxygen isotope ranking of late Eocene and Oligocene planktonic foraminifers—Implications for Oligocene sea-surface temperatures and global ice-volume, *Mar. Micropaleontol.*, *9*, 111–134.

Poulsen, C. J., E. J. Barren, W. H. Peterson, and P. A. Wilson (1999), A reinterpretation of mid-Cretaceous shallow marine temperatures through model-data comparison, *Paleoceanography*, *14*, 679–697.

Poulsen, C. J., E. J. Barron, M. A. Arthur, and W. H. Peterson (2001), Response of the mid-Cretaceous global oceanic circulation to tectonic and CO_2 forcings, *Paleoceanography*, *16*, 576–592.

Price, G. D., B. W. Sellwood, R. M. Corfield, L. Clarke, and J. E. Cartlidge (1998), Isotopic evidence for palaeotemperatures and depth stratification of Middle Cretaceous planktonic foraminifera from the Pacific Ocean, *Geol. Mag.*, *135*, 183–191.

Rao, Y. H., C. Subrahmanyam, S. R. Sharma, A. A. Rastogi, and B. Deka (2001), Estimates of geothermal gradients and heat flow from BSRs along the Western Continental Margin of India, *Geophys. Res. Lett.*, *28*, 355–358.

Reichart, G. J., F. Jorissen, P. Anschutz, and P. R. D. Mason (2003), Single foraminiferal test chemistry records the marine environment, *Geology*, *31*, 355–358.

Rosenthal, Y., G. P. Lohmann, K. C. Lohmann, and R. M. Sherrell (2000), Incorporation and preservation of Mg in Globigerinoides sacculifer: Implications for reconstructing the temperature and $\delta^{18}O$ of seawater, *Paleoceanography*, *15*, 135–145.

Rudnicki, M. D., P. A. Wilson, and W. T. Anderson (2001), Numerical models of diagenesis, sediment properties, and pore fluid chemistry on a paleoceanographic transect: Blake Nose, Ocean Drilling Program Leg 171B, *Paleoceanography*, *16*, 563–575.

Savin, S. M. (1977), The history of the Earth's surface temperature during the past 100 million years, *Annu. Rev. Earth Planet. Sci.*, *5*, 319–355.

Scholle, P. A., and M. A. Arthur (1980), Carbon isotope fluctuations in Cretaceous pelagic limestones: potential stratigraphic and petroleum exploration tool, *AAPG Bull.*, *64*, 67–87.

Schrag, D. P. (1999), Effects of diagenesis on the isotopic record of late Paleogene tropical sea surface temperatures, *Chem. Geol.*, *161*, 215–224.

Schrag, D. P., D. J. DePaolo, and F. M. Richter (1995), Reconstructing past sea-surface temperatures—Correcting for diagenesis of bulk marine carbonate, *Geochim. Cosmochim. Acta*, *59*, 2265–2278.

Sexton, P. F. (2005), Foraminiferal palaeoecology and palaeoceanography of the Eocene, Ph.D. thesis, 208 pp, Natl. Oceanogr. Cent., Univ. of Southampton, Southampton, U. K.

Sexton, P. F., P. A. Wilson, and P. N. Pearson (2006), Palaeoecology of late middle Eocene planktic foraminifera and evolutionary implications, *Mar. Micropaleontol.*, *60*, 1–16.

Shackleton, N., and A. Boersma (1981), The climate of the Eocene ocean, *J. Geol. Soc.*, *138*, 153–157.

Shackleton, N. J., R. M. Corfield, and M. A. Hall (1985), Stable isotope data and the ontogeny of Paleocene planktonic foraminifera, *J. Foraminiferal Res.*, *15*, 321–336.

Shellito, C. J., L. C. Sloan, and M. Huber (2003), Climate model sensitivity to atmospheric CO_2 levels in the Early-Middle Paleogene, *Palaeogeogr. Palaeoclimatol. Palaeoecol.*, *193*, 113–123.

Sloan, L. C., and E. J. Barron (1992), A comparison of Eocene climate model results to quantified paleoclimatic interpretations, *Palaeogeogr. Palaeoclimatol. Palaeoecol.*, *93*, 183–202.

Sloan, L. C., and D. K. Rea (1996), Atmospheric carbon dioxide and early Eocene climate: A general circulation modeling sensitivity study, *Palaeogeogr. Palaeoclimatol. Palaeoecol.*, *119*, 275–292.

Sorby, H. C. (1879), Structure and origin of limestone: Anniversary address of the President, *Geol. Soc. London. Q. J.*, *35*, 56–95.

Spero, H. J. (1998), Life history and stable isotope geochemistry of planktonic foraminifera, in *Isotope Paleobiology and Paleoecology*, edited by R. D. Norris and R. M. Corfield, pp. 7–36, Paleontol. Soc., Pittsburgh, Pa.

Spero, H. J., and D. W. Lea (1993), Intraspecific stable-isotope variability in the planktic foraminifera *Globigerinoides sacculifer*—Results from laboratory experiments, *Mar. Micropaleontol.*, *22*, 221–234.

Spero, H. J., and D. W. Lea (1996), Experimental determination of stable isotope variability in *Globigerina bulloides*: Implications for paleoceanographic reconstructions, *Mar. Micropaleontol.*, *28*, 231–246.

Spero, H. J., and D. F. Williams (1989), Opening the carbon isotope "vital effect" black box: 1. Seasonal temperatures in the euphotic zone, *Paleoceanography*, *4*, 593–601.

Spero, H. J., I. Lerche, and D. F. Williams (1991), Opening the carbon isotope "vital effect" black box: 2. Quantitative model for interpreting foraminiferal carbon isotope data, *Paleoceanography*, *6*, 639–655.

Spero, H. J., J. Bijma, D. W. Lea, and B. E. Bemis (1997), Effect of seawater carbonate concentration on foraminiferal carbon and oxygen isotopes, *Nature*, *390*, 497–500.

Stott, L. D., J. P. Kennett, N. J. Shackleton, and R. M. Corfield (1990), The evolution of Antarctic surface water during the Palaeogene: Inferences from the stable isotopic composition of planktonic foraminifera, ODP Leg 113, *Proc. Ocean Drill. Program Sci. Results*, *113*, 849–863.

Tajika, E. (1998), Climate change during the last 150 million years: Reconstruction from a carbon cycle model, *Earth Planet. Sci. Lett.*, *160*, 695–707.

Tripati, A. K., M. L. Delaney, J. C. Zachos, L. D. Anderson, D. C. Kelly, and H. Elderfield (2003), Tropical sea-surface temperature reconstruction for the early Paleogene using Mg/Ca ratios of planktonic foraminifera, *Paleoceanography*, *18*(4), 1101, doi:10.1029/2003PA000937.

Veizer, J., et al. (1999), $^{87}Sr/^{86}Sr$, $\delta^{18}C$ and $\delta^{18}O$ evolution of Phanerozoic seawater, *Chem. Geol.*, *161*, 59–88.

Wade, B. S., and D. Kroon (2002), Middle Eocene regional climate instability: Evidence from the western North Atlantic, *Geology*, *30*, 1011–1014.

Wallmann, K. (2001), Controls on the Cretaceous and Cenozoic evolution of seawater composition, atmospheric CO_2 and climate, *Geochim. Cosmochim. Acta*, *65*, 3005–3025.

Wilkinson, B. H., and T. J. Algeo (1989), Sedimentary carbonate record of calcium magnesium cycling, *Am. J. Sci.*, *289*, 1158–1194.

Wilson, P. A., and R. D. Norris (2001), Warm tropical ocean surface and global anoxia during the mid-Cretaceous period, *Nature*, *412*, 425–429.

Wilson, P. A., and B. N. Opdyke (1996), Equatorial sea-surface temperatures for the Maastrichtian revealed through remarkable preservation of metastable carbonate, *Geology*, *24*, 555–558.

Wilson, P. A., R. D. Norris, and M. J. Cooper (2002), Testing the Cretaceous greenhouse hypothesis using glassy foraminiferal calcite from the core of the Turonian tropics on Demerara Rise, *Geology*, *30*, 607–610.

Winland, H. D. (1969), Stability of calcium carbonate polymorphs in warm, shallow water, *J. Sediment. Petrol.*, *39*, 1579–1587.

Zachos, J., M. Pagani, L. Sloan, E. Thomas, and K. Billups (2001), Trends, rhythms, and aberrations in global climate 65 Ma to present, *Science*, *292*, 686–693.

Zachos, J. C., L. D. Stott, and K. C. Lohmann (1994), Evolution of early Cenozoic marine temperatures, *Paleoceanography*, *9*, 353–387.

Zachos, J. C., M. W. Wara, S. Bohaty, M. L. Delaney, M. R. Petrizzo, A. Brill, T. J. Bralower, and I. Premoli-Silva (2003), A transient rise in tropical sea surface temperature during the Paleocene-Eocene Thermal Maximum, *Science*, *302*, 1551–1554.

Zeebe, R. E. (1999), An explanation of the effect of seawater carbonate concentration on foraminiferal oxygen isotopes, *Geochim. Cosmochim. Acta*, *63*, 2001–2007.

Zimmermann, H. (2000), Tertiary seawater chemistry—Implications from primary fluid inclusions in marine halite, *Am. J. Sci.*, *300*, 723–767.

Zwart, G., J. C. Moore, and G. R. Cochrane (1996), Variations in temperature gradients identify active faults in the Oregon accretionary prism, *Earth Planet. Sci. Lett.*, *139*, 485–495.